UNIVERSITÀ
POLITECNICA
DELLE MARCHE

DEPARTMENT OF ENGINEERING

Master's Degree in Biomedical Engineering

A Finite Element Analysis for the assessment of Tibial Internal and External Rotation: effects in Healthy Knee

Supervisor:

Prof. Marco Mandolini

Candidate:

Alessia Ortolani

Co-supervisors:

Prof. Lorenzo Scalise

Prof. Antonio Pompilio Gigante

Academic Year 2021-2022

A chi ci ha creduto, insieme a me.

I. Contents

II. List of figures

III. List of tables

Abstract

The knee represents the biggest and most complex human joint and still nowadays many aspects related to the maintenance of its functionality need to be investigated. The wear of the cartilage part could bring to a disease known as osteoarthritis that provoke knee pain which can be related to the femoral-tibial misalignment. This disease can be treated with the use of prostheses to restore the normal knee function. However, it is known that the misalignment of the prosthetic components can cause greater wear of the polyethylene insert, thus leading to an early revision. Moreover, it has been observed that patients with tibia internal rotation had a correlation with the development of osteoarthritis. Finally, it has been seen that elderly people with healthy knee present instead a tibia external rotation. Until now, no studies have been conducted on different femoral-tibial torsion configurations in healthy knee. For this reason, the current study aims to develop and compare two healthy knee models that present respectively a femoral-tibial torsion of -11° and 0°, by means of Finite Element Analysis (FEA). Therefore, the purpose is to determine if in a virtual knee prototype the internal rotation of the tibia causes higher stress values during flexion. The results seem to be promising, in fact it has been found that the internal rotation of the tibia causes greater stress in the menisci, in particular in the medial part. Despite the stress in the tibia appears to be greater in the tibia external rotation case, this seems to be spread over a more extensive area in the internal rotation case which is also comparable with the wear present in a real tibia with osteoarthritis (OA). Thus, this seems to confirm the correlation between the internal rotation of the tibia with OA development. It can be concluded that the finite element model employed in this work can study the effects that different femoral-tibial torsion conditions provoke on the knee. Thus, this study can be considered as a first step towards new research that aims to computationally determine the benefits that preventive osteotomy could bring.

Riassunto

Il ginocchio rappresenta l'articolazione più grande e complessa e ancor oggi molti aspetti legati al mantenimento delle sue funzionalità devono essere approfonditi. L'usura della parte cartilaginea porta ad una malattia nota come osteoartrite che provoca dolore al ginocchio e che può essere ricondotta al disallineamento tra femore e tibia. Questa malattia può essere trattata attraverso l'impiego di protesi per ristabilire il normale funzionamento del ginocchio. È risaputo però che il disallineamento delle componenti protesiche può provocare maggiore usura dell'inserto in polietilene e quindi un precoce bisogno di revisione. Inoltre, è stato osservato che i pazienti che presentano una rotazione interna della tibia hanno una correlazione con lo sviluppo dell'osteoartrite. Infine, è stato visto che soggetti anziani con ginocchio sano presentano invece una rotazione esterna della tibia. Ad oggi nessuno studio è stato condotto su diverse configurazioni di torsione femoro-tibiali in ginocchi sani. Per questo motivo il presente studio ha lo scopo di sviluppare e comparare due modelli di ginocchio sano che presentano rispettivamente una torsione femore-tibiale di -11° e 0°, attraverso l'analisi agli elementi finiti (FEA). Dunque, si è voluto determinare se in un modello virtuale di ginocchio la rotazione interna della tibia provoca durante la flessione valori di stress maggiori. I risultati ottenuti sembrano incoraggianti, si è trovato infatti che la rotazione interna della tibia provoca maggiore stress nei menischi, in particolare nella parte mediale. Sebbene il valore di stress nella tibia risulti essere maggiore nel caso con rotazione esterna, questo appare essere diffuso in un'area più estesa nel caso con rotazione interna risultando inoltre comparabile con l'usura presente in una tibia reale con osteoartrite. Ciò sembra confermare quindi la correlazione tra rotazione interna della tibia e osteoartrite. Si può dedurre dunque che il modello agli elementi finiti impiegato in questo lavoro può studiare gli effetti che diverse condizioni di torsione femoro-tibiali provocano sul ginocchio. Questo studio può essere considerato come un primo passo verso una nuova ricerca finalizzata alla determinazione computazionale dei benefici dell'osteotomia preventiva.

1 Introduction

The knee represents the largest and most complex joint that connects the femur, tibia and patella by means of two articulations: the tibiofemoral (TF) and patellofemoral (PF) joints. It is characterized by six degree of motions, three displacements and three rotations [1]. Despite this, due to its hinged joint nature, it mainly allows movement along the flexion/extension axis in the sagittal plane. In the full extension position, the knee is locked by the so called screw-home mechanism which consists in the internal rotation of the tibia or external rotation of the femur during the flexion. For this reason, a slight medial rotation is also possible, as well as the antero-posterior translation due to the characteristic roll-back movement. The knee osteoarthritis (OA), which is a degenerative knee joint disease that may lead to disability, is the result of wear and tear representing a progressive loss of articular cartilage. The clinical symptoms vary among each individual. However, they usually become more severe and debilitating over time. Common clinical symptoms are knee pain, which is gradual in onset and became worsen with activity, knee stiffness and swelling. For this reason, over the last 40 years, several surgical techniques, including total knee arthroplasty (TKA), have been developed and implemented to reduce knee pain and restore kinematics to patients suffering from osteoarthritis and chronic pain in the knee. In fact, TKA is recognized as an effective and successful treatment for end-stage knee osteoarthritis, even though up to 20% of patients report unsatisfaction and knee pain in post-surgery. It is well known that one of the causes are related to the malalignment of the prosthesis components [2]. In fact, knee surgeons learned from TKA procedures that a malposition of the implants due to axial or rotational misalignment can result in higher revision rate [3][4]. In particular, an early revision is required in case of polyethylene wear, knee instability, loosening and infection [5]. Moreover, orthopaedists observed that higher wear was present in the medial part of the polyethylene insert in case of tibial component internal rotation in knees that undergo TKA procedure [6]. This observation can be linked to pain and difficulties

in performing daily activities caused by the excessive internal component rotation. Thus, surgeons try to compensate this problem placing the components in sight external rotation since it seems to be well tolerated by the patients [7].

The paper of [8] reports a similar observation in a pre-surgical knee. In this case, it has been examined the correlation between gait changes after Anterior Cruciate Ligament (ACL) injury and the progression of knee OA. In particular, a tibial internal rotation has been reported to occur during walking in patients with ACL-deficient knees. This reveals a greater rate of cartilage loss in the medial compartment relative to the lateral, resulting in a drift in a varus alignment.

Consequently, the alignment of human lower limb has represented an area of ongoing study for decades. Nowadays, the definition of "normal axial and rotational alignment" in non-arthritic subjects remains not fully clear. From the previous observations, it comes that the rotational alignment, referred as the angle between the transepicondylar axis (TEA) and the posterior tangent to tibia (PTT), represents an important aspect for the maintenance of knee functionality. Hence, a femoral-tibial torsion (TEA-PTT) out of normal range can alter the loading distribution in the knee joint [4]. And this, having a direct effect on the transmitted load, leads to the increase of cartilage wear and thus OA development [3][9].

A recent study [10] highlighted a significant difference in terms of proximal tibia anatomy between non-arthritic and OA knees. The non-arthritic subjects presented a femoral-tibial torsion between -3° and 0.9°, while the OA ones reported a tibia internal rotation between -16° and -9.1°. Thus, it has been found a significant internal rotation of tibial plateau in OA knees compared with healthy ones. In this scenario, the Finite Element Analysis (FEA) has made its way allowing a detailed analysis of the joint behaviour. Indeed, FEA is considered a useful tool to predict strain and stress in complicated systems in bioengineering and biomechanics [11]. However, usually several assumptions have been made to simplify the knee behaviour, thus making the knee model less realistic [12]. Since the results accuracy in FE model depends directly on assumptions made in the model, an anatomically accurate design could increase the possibility to obtain a more realistic simulation of the complex knee joint

biomechanics. Then FEA can be recognized as a reliable tool to investigate the biomechanical behaviour of healthy knees. It can also be used to assess the eventual onset of some pathologies, like OA, and consequently understand if the performance of the TKA is required. However, despite the FEA has been largely applied in the study of the human knee kinematics, its implementation for the exploration of rotational malalignment in healthy knee has not been performed yet. For this reason, it could be useful to determine if in a virtual knee prototype the tibial internal rotation cause higher stress and consequently understanding if a preventive knee osteotomy, which consists in the external rotation of the tibia, could delay the OA occurrence and thus the prosthesis implantation and revision. So, FEA performed on different configurations could be useful to determine the stress improvement that osteotomy could bring.

Considering this, the current study aims to develop two 3D finite element knee models to study the effects of different femoral-tibial configurations in healthy knees. In particular, a model with a tibial internal rotation of -11° and one with an external rotation of 0°, that represents the normal configuration, have been developed and compared to confirm the orthopaedist observations using FEA.

2 Human knee joint

This section will treat the human knee joint in detail. The description of the anatomy (Section 2.1) will then be followed by the description of the TF biomechanics (Section 2.2). In particular there will be the explanation of the complex knee movement which is strictly related to the knee joint alignment. As previously described, a misalignment of the knee could be correlated with the development of OA. For this reason, in Section 2.3 the description of OA and its treatment can be found.

2.1 Anatomy

The knee is the largest joint of the human body and exhibits very complex kinematics. Despite its significant mobility, it has great stability thanks to the presence of the surrounding ligament structure. It is a compound joint, formed by four bones and a complex structure of soft tissues. The bones involved are the distal femur (thigh bone), the proximal tibia (shin bone), the patella (kneecap) and the proximal apex of the fibula. The soft tissues instead consist of fibrous capsule, synovial membrane, two menisci, ligaments and numerous bursae Figure 2.1.

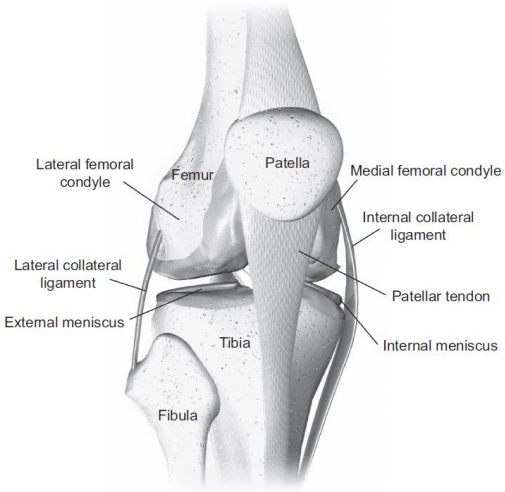

Figure 2.1 Knee components.

2.1.1 Bones

The knee joint is located between the two longest bones of the human body which are the femur and the tibia. Therefore, high moments are often generated making it vulnerable and susceptible to frequent injuries. The knee is considered as a compound of two joints, the tibiofemoral and the patellofemoral one (Figure 2.2).

Figure 2.2 Knee joint bone structure.

The distal femur is made by two condyles, lateral and medial, which represent the articular surface of the thigh bone and act approximately as two rolling spheres or cylinders, allowing the interaction with the tibia along the flexion-extension axis. Condyles are divided by the trochlear groove that guides patella translation during knee motion, and they are characterized by an asymmetrical geometry. In fact, the lateral condyle is ball-shaped, distally less rounded and has a smaller posterior offset, while the medial one is elliptical and more distal than lateral, with a circular posterior condyle and a larger posterior offset. The posterior offset is defined as the distance between the posterior part of the femur and the posterior part of the tibia [13].

The condyles are anatomically multiple radius shaped, because of their radius of curvature that decreases going from the anterior to the posterior area. This feature influences the behaviour of the femur during the motion of the knee. The successive centres of curvatures do not coincide, but they create a J-curve that determines the variation of the ratio between the rolling and the sliding (Figure 2.3).

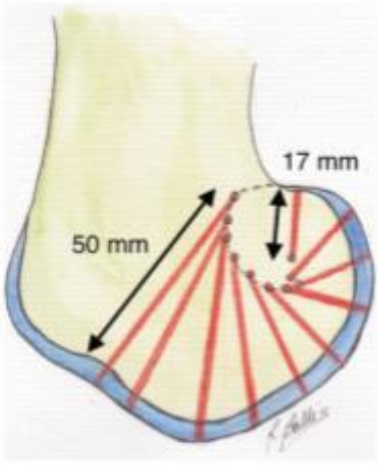

Figure 2.3 J-curve of the femoral condyles.

The proximal tibia is composed of two asymmetric plateaus, medial and lateral, divided by the intercondylar eminence (lateral and medial tubercles) (Figure 2.4). The medial plateau is 50% larger and 3 times thicker than the lateral one, thus matching with the dimensions of the medial femoral condyle. It is also more oval and shows a concave articular surface in the anterior-posterior direction allowing a wider lateral mobility. The lateral plateau is smaller, more rounded and its articular surface is convex in the anterior-posterior direction [14].

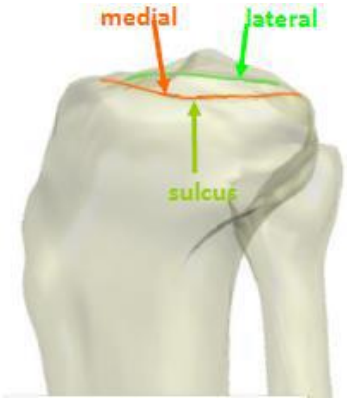

Figure 2.4 Tibial plateaus.

A significant characteristic of the tibial plateau is related to its posterior slope of around 10° (with the anterior elevation being higher than the posterior one). This inclination facilitates the flexion-extension mechanism of the knee, by making the lateral sliding of the bones easier [14].

Finally there is the patella (or kneecap), a hard triangular-shaped bone which is situated in the intercondylar notch and embedded in the tendon of the quadriceps femoris muscle above and the patella tendon below. It shows two flat articular surfaces (medial and lateral facets) and its posterior surface is covered with cartilage to smooth the contact with the patellar groove of the femur (Figure 2.5). In fact, it is involved in the PF joint, a low friction sliding articulation that moves the patella caudally during flexion allowing thus its sliding in the patellofemoral groove. The primary kneecap role is to transmit the forces of the extensor mechanism, but it also increases the lever arm of the knee to reduce forces. Moreover, it is responsible for the prevention of anterior-posterior tibiofemoral shear stresses that can be the cause of dislocations.

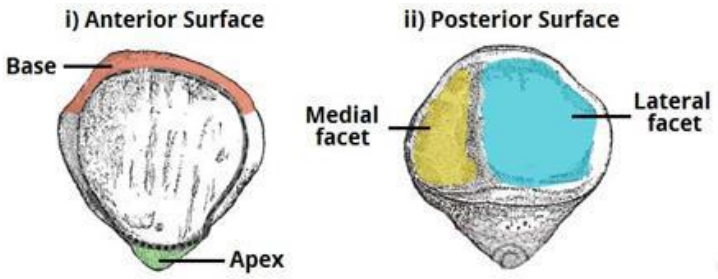

Figure 2.5 Anterior and posterior surfaces of the patella.

2.1.2 The cartilage

Cartilage is a thin and elastic tissue that cover the tibial plateaus, the femoral condyles, the patellar groove and the posterior surface of the patella (Figure 2.6). In the knee, there are two types of cartilage: the fibrous one, that mainly composes the menisci and is characterized by a significant tensile and compressive strength, and the hyaline one, covering the surface along which the joints move. Its presence increases the area of contact of the articular surfaces for a more homogeneous distribution of the

forces on the bones. It also makes the sliding motion between bones smoother, almost frictionless, and acts as a shock absorber. The smooth contact is important to avoid the deterioration of the underlying bone. The nerves and vessels do not achieve this part, therefore it is not possible to detect a possible damage until a bone rubs against another one. Cartilage is subjected to wear over the years and has a very limited capacity of self-restoration. Indeed, the newly formed tissue after damage generally consists of fibrous tissue in a lower amount respect to the original one, resulting then in the formation of new cracks and tears over time.

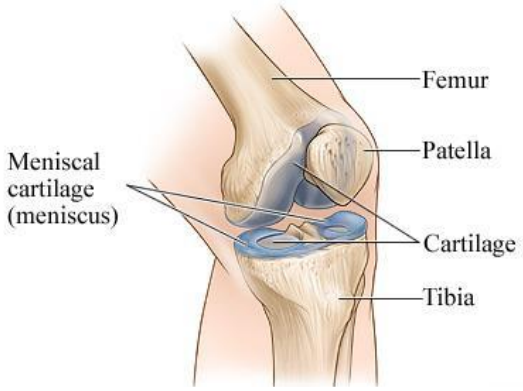

Figure 2.6 Cartilaginous structures in the knee.

2.1.3 Menisci

The menisci are two crescent-shaped fibrocartilaginous structures (medial and lateral) that accept the convex femoral condyle superiorly and the peripheral tibial plateau inferiorly. They have a crucial role in the improvement of joint congruence between the femoral condyles and tibial plateau, in the proprioception of the knee joint and in the transmission of loads by increasing the TF contact area thus protecting cartilage from excessive axial stresses [15]. Without them, the nonconformity between the femoral condyles and tibial plateaus would lead to increased contact stress during motion, causing consequently the onset of the complications [13]. They consist of connective tissues with collagen fibers that are mainly arranged circumferentially and crossed by radial fibers to improve meniscal strength and rigidity. The peripheral section is thick and convex while the central part is thin. Since the medial meniscus receives a greater blood supply than the lateral one, the injuries involving the lateral

meniscus require longer rehabilitation. In addition, the lateral meniscus is more mobile than the medial one [13]. The menisci are made of three segments: anterior horn, posterior horn, and body. At the lateral meniscus, the horns have the same sizes, while at the medial meniscus, the posterior horn is larger than the anterior one. The medial meniscus is generally semicircular, larger, and thicker than the lateral and measures approximately 3.5 cm. It matches the medial tibial plateau shape. Instead, the lateral meniscus is almost circular and covers a larger portion of the lateral tibial plateau. It is much more mobile than the medial meniscus in fact it has the ability to move 1 cm anteroposterior and laterally (Figure 2.7).

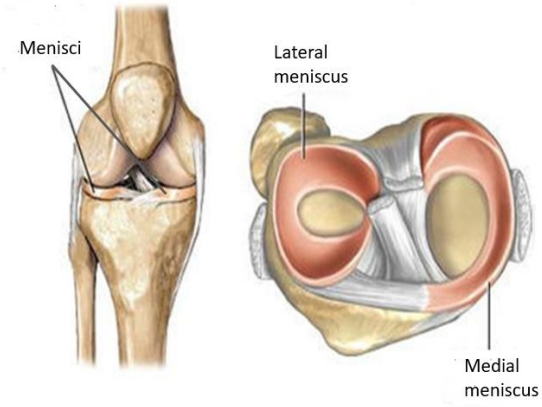

Figure 2.7 Menisci: frontal view (left) and top view (right).

2.1.4 Ligaments

The knee stability is achieved thank to the primary and secondary stabilizers. Primary knee stabilization is provided by knee ligaments, while the secondary one is performed by the muscles [13]. The ligaments consist of closely packed collagen fiber bundles that provide support to the joint articulation and prevent excessive movements [16]. The most important are the cruciate and collateral ligaments (Figure 2.8). The cruciate ligaments are localized within the capsule and are surrounded by a synovial layer. They connect the femur and the tibia crossing each other obliquely, hence from this it comes the term "cruciate". They are divided into the anterior cruciate ligament (ACL) and posterior cruciate ligament (PCL), according to their site of attachment to the tibia. The ACL arises from the anterior part of the intercondylar

eminence of the tibia and extends to the posterolateral aspect of the intercondylar fossa of the femur. It consists of two bundles, an anteromedial (AM) and a posterolateral (PL) bundle [17]. The AM bundle is a restraint to anterior-posterior translation of the knee, while the PL bundle is an important limitation to rotational moments of the knee. During passive flexion the AM bundle is stretched, while the PM one stretches during passive extension movement. The principal role of ACL is to limit excessive anterior translation of the tibia and excessive posterior translation of the femur. It is considered the main stabilizer of the knee since it contributes to about 85% of the knee stabilization and allows smooth and steady flexion and rotation of the knee. The PCL instead rises from the posterior part of the intercondylar eminence of the tibia and moves to the anterolateral aspect of the intercondylar fossa of the femur. Its main function is to withstand an excessive anterior femoral translation or an excessive posterior tibial translation. Also the PCL is composed of two bundles, the anterolateral (AL) and the posteromedial (PM) bundle [18]. Instead for what concerns the collateral ligaments, they ensure joint stability in the mediolateral direction and prevent undesired motion. They include the medial collateral ligament (MCL) and the lateral collateral ligament (LCL). MCL stabilizes the medial surfaces of the knee, minimizing the valgus and internal rotation during flexion. While LCL stabilize the lateral surface of the distal femur to the proximal fibula preventing excessive varus stress and external rotation at all positions of knee flexion [18].

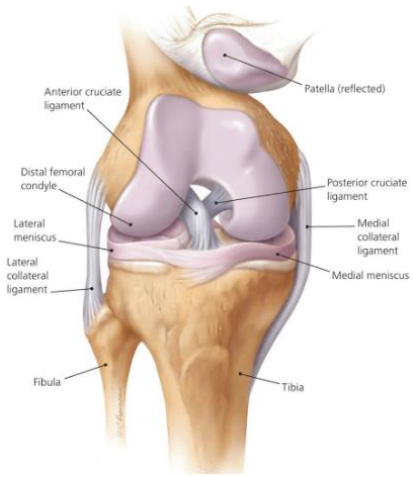

Figure 2.8 Knee ligaments.

2.1.5 Synovial capsule

The synovial capsule is a closed cavity containing the synovial fluid which is a lubricant that has a low coefficient of friction (Figure 2.9). It allows the sliding and rotation of the tibial cartilage with respect to the femoral cartilage, especially with the presence of high forces. Thus, thanks to the synovial fluid the backbone of the knee moves with minimal resistance [13].

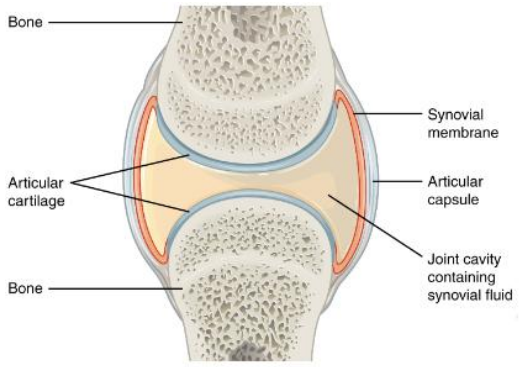

Figure 2.9 Synovial capsule

.

2.1.6 Muscles

The secondary stabilizers of the knee joint are the muscles. Their primary function is to produce knee motion, but they can also interact with the neuromuscular system to control the motion [13]. Specifically, the stabilization and the movement of the knee in flexion and extension are guaranteed by two main muscle groups in the leg which are the hamstring and quadriceps muscle. The quadricep consists of four muscles: rectus femoris, vastus lateralis, vastus medialis, and vastus intermedius. These are attached to the proximal part of the tibia through the quadriceps tendon and through the patellar tendon inserts to the tibia (Figure 2.10). The quadriceps produce a force that not only permits the extending moment in the knee but also guarantee together with the patellar tendon, that the patella is kept in the trochlear groove of the femur.

On the other side, the hamstring consists of three muscles: semitendinosus, semimembranosus, and biceps femoris muscle. These muscles run along the back part of the femur and attach to the fibula and tibia to flex the knee (Figure 2.10).

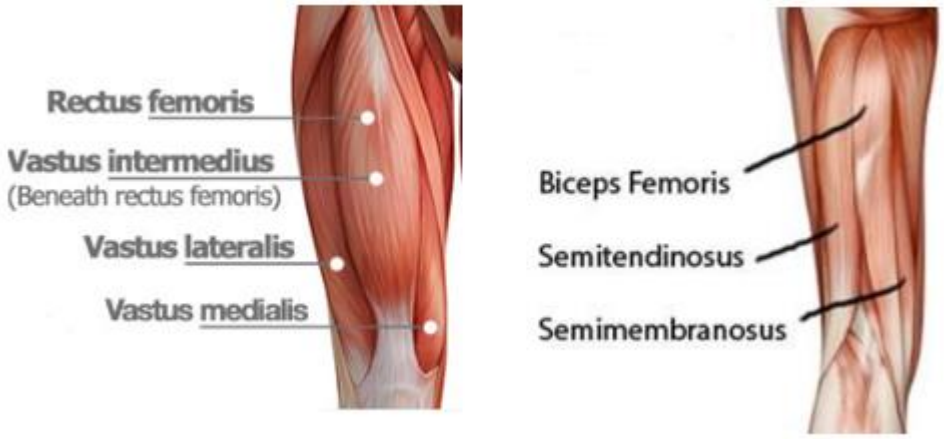

Figure 2.10 Quadricep (left) and hamstring (right).

2.1.7 Tendons

Tendons are structures that join muscles and bones and transmit the forces produced by the muscles to bones allowing the knee joint movement. In particular, the quadriceps act to extend the knee through the quadriceps patellar tendon mechanism, indeed the quadriceps tendon fibers extend across the anterior surface of the patella and blend distally with the patellar tendon.

This last one is one of the strongest collagenous structures of the body and it is designed for the transmission of high tensile loads and to keep the patella close to a constant distance from the tibia. In addition, the medial and lateral hamstrings act to flex the knee through their respective tendons. Furthermore, the iliotibial band performs a counterbalanced activity to the knee adduction moment, ensuring lateral stabilization [13].

2.2 Tibiofemoral biomechanics

The tibiofemoral joint is an articulation between the lateral and medial condyles of the distal end of the femur and the tibial plateaus, both of which are covered by a thick layer of hyaline cartilage. The articular surfaces of the tibiofemoral joint are generally incongruent, so compatibility is provided by the medial and lateral meniscus.

2.2.1 Movement

Kinematics is the quantitative study of motion. The knee joint is characterized by six degrees of freedom (DOF), three rotations and three translations along a set of perpendicular axes (Figure 2.11).

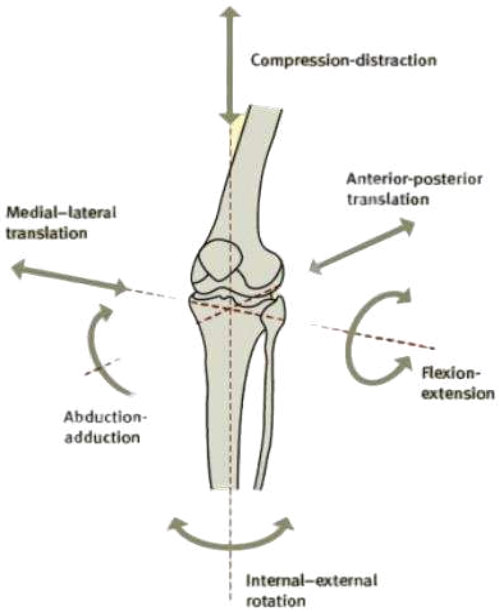

Figure 2.11 Six degrees of motion.

The principal movements are respectively the flexion/extension, the internal/external rotation and anterior/posterior translation, while the minor ones are usually restrained by ligaments and are the varus/valgus rotations, the medial/lateral and the compression/distraction translations. In particular, the knee allows a flexion movement up to 160° from a standing up configuration of 5° of hyperextension. In full extension the knee is locked by the screw-home mechanism, which allows the maintenance of this position with minimal energy output [19].

This configuration depends on two main forces: the ground reaction force (GRF) on one side and the tension of the ligaments on the other, allowing the leg to support the whole body weight in the upright position, without any muscular activity. The flexion is a combination of rolling and gliding which can be referred as the so called "roll-back" movement [20] (Figure 2.12).

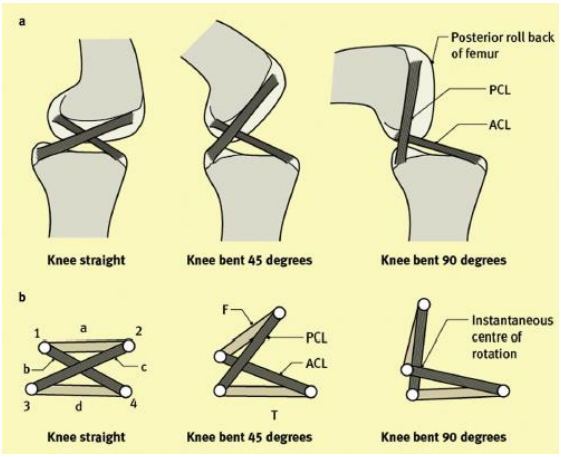

Figure 2.12 Knee joint kinematics in the sagittal plane: roll-back movement.

The four-bar link mechanism, formed by the cruciate ligaments together with the femur and tibia, contribute to posterior femoral roll back, causing a posterior translation of the instantaneous centre of rotation of knee joint as the flexion increase, thus preventing soft tissue impingement [21]. This means that if the flexion was a pure roll motion, the femur would roll off the tibial plateau before the knee reaches full flexion. Following Figure 2.12, at full extension the femur has a large contact area with the tibial plateaus and pushes anteriorly on the meniscal horns. As the knee starts to flex, the contact moves posteriorly towards the posterior meniscal horns and the TF contact area is reduced since lower femoral condyles radii are sequentially coming into contact [1]. During the flexion, a tibial internal rotation (up to approximately 15°) around a medial pivot point occurs, representing the reverse of the screw-home mechanism. This happens because the medial tibial plateau is slightly concave while the lateral one is flat, meaning that the centre of contact in the medial side remains relatively constant in terms of AP position, instead the lateral condyle rolls posteriorly towards the posterior horn of the lateral meniscus [1]. Finally in deep flexion, when

the ACL is in tension it allows to resist to a further posterior translation of the TF contact point, so the femur slides anteriorly and rolls posteriorly at the same time [22].

2.2.2 Alignment

The forces acting on the knee joint depends on the alignment of its components and on the musculotendinous structures. The axes can be divided into mechanical and anatomical axis. The lower limbs mechanical axis can be determine drawing a straight line from the centre of the femoral head to the centre of the ankle (Figure 2.13). In particular, the femoral mechanical axis goes from the centre of the femoral head to the one of the intercondylar region. Instead, the mechanical axis of the tibia passes through the centre of the tibial plateau to the centre of the ankle joint.

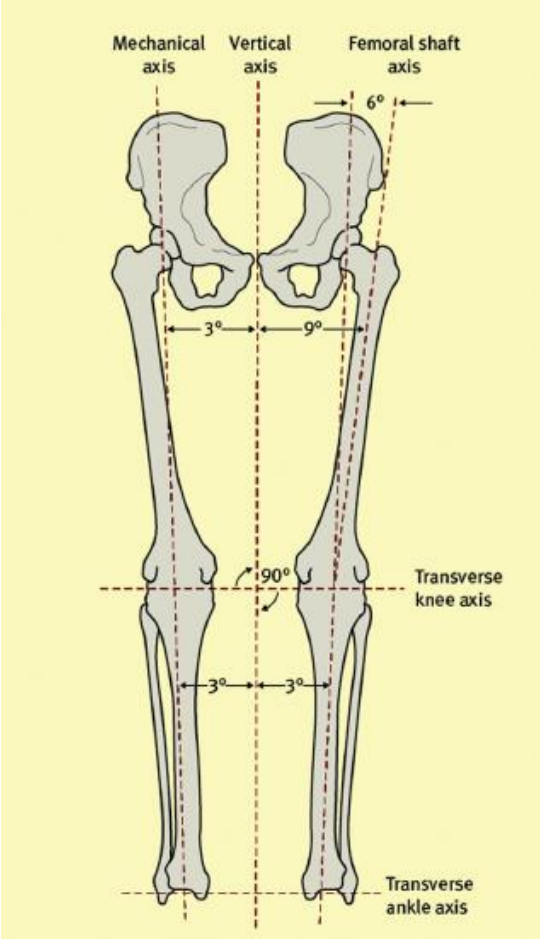

Figure 2.13 Anatomical and mechanical axis of the lower limb in coronal plane.

As can be appreciated from Figure 2.13, the mechanical axis of the lower limb is not parallel to the vertical line that passes by the symphysis pubis. In fact, it makes an angle of 3° with it, meaning that the transverse knee axis, which is perpendicular to the vertical line, is in 3° of varus in relation to the mechanical axis. For what concerns the anatomical axis of the femur and tibia, these are lines drawn along their medullary canals. In the tibia, the anatomical and mechanical axis overlap each other, while in the femur they form an angle of 5°-7° in the coronal plane. Consequently, the anatomical axis of the femur makes an angle of 8°-10° with the vertical line. In the sagittal plane instead, the articular surface of the tibia has a posterior slope. This can be measured by the angle between the anatomical axis of the tibia and a line drawn along the tibial plateau. This slope is around 6°-9° but it is reduced by the wedge-shaped meniscus. In a cruciate retaining prosthesis, it is essential to recreate this slope to ensure the roll back movement of the femur. Another key alignment is related to the rotational alignment. This is important since it affects tibiofemoral and patellofemoral kinematics, but also the flexion alignment and stability. The reference lines used to measure the femoral rotation include the transepicondylar axis (TEA), the Whiteside line and the posterior condylar line of femur (PCA) (Figure 2.14).

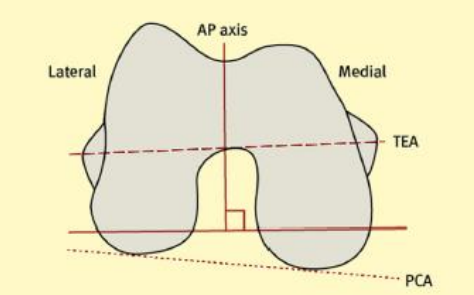

Figure 2.14 Transepicondylar axis (TEA), the Whiteside line and the posterior condylar line of femur (PCA).

The TEA is defined by anatomic landmarks and is a mechanical axis around which femoral rotation occurs. Since the epicondyles are the attachment sites of the collateral ligaments, this line is also an important reference for soft tissue balancing. The Whiteside line can be drawn from the deepest part of the trochlear grove anteriorly to

the centre of the intercondylar notch posteriorly, and it is almost perpendicular to the TEA. The PCA of the femur can also be used as a reference line and makes an angle of 3° with the TEA. When the knee is in the flexion position, this neutralizes the 3° varus of the tibial articular surface in the coronal plane, allowing the TEA to remain parallel to the tibial articular surface. However, this line can be easily affected by arthritic changes, thus is less reliable.

The rotational alignment of the tibia instead is measured by drawing a medial to lateral line connecting the widest point of the tibial articular surface. An anteroposterior axis perpendicular to this line is used for reference. The posterior condylar line tangent to the tibia (PTT) (Figure 2.15) and the transmalleolar axis are other anatomical references used for assessing rotational alignment of the tibia.

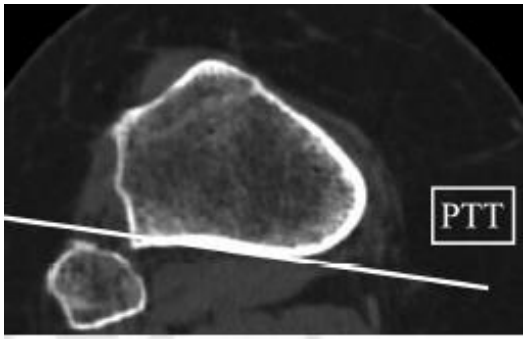

Figure 2.15 Posterior condylar line tangent to the tibia (PTT).

In particular, the femoral-tibial torsion, which is the angle between TEA and PTT, can be evaluated to determine the TF rotational alignment (1). This is an important aspect since several studies have documented that a TF joint malalignment can cause alterations in the knee biomechanics, being also correlated with OA development.

2.3 Osteoarthritis and treatment

Knee osteoarthritis (OA) is the progressive degeneration and wear of the meniscus and articular cartilage of the knee [23] (Figure 2.16).

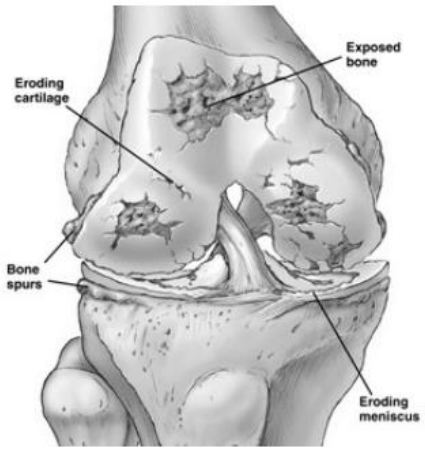

Figure 2.16 Knee cartilage wear due to osteoarthritis (OA).

It can be related to the defect in the cellular replacement process of chondrocytes which are the main cells that form the articular cartilage matrix. In fact, the dynamic equilibrium between the formation and breakdown of the cartilaginous matrix is regulated by an interplay of anabolic and catabolic influences. These mechanisms are useful to compensate for the harmful effects of OA by stimulating and modifying the metabolic activity of chondrocytes. Matrix degradation occurs when these harmful effects exceed the system ability to compensate cartilage degradation [24].

The articular cartilage loss in OA may start as a focal lesion and then progressively extend to involve specific compartments, so inducing alterations in articulating surfaces and leading to a further loss of cartilage. This degeneration cause then functionality loss and knee pain. In particular, this leads to a change in the meniscus shape and articulating surfaces. The meniscus that served as pressure distributor over the articulating surfaces lose its function and pressure points are created (Figure 2.17).

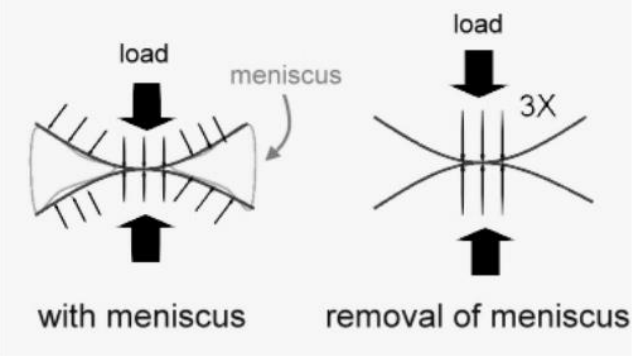

Figure 2.17 Effect of meniscus loss.

These pressure points cause additional wear upon the articular cartilage and pain during loading and motion.

Nowadays OA is not a curable disease since the mechanism by which it arises and progresses remains unclear. Therefore, the treatments aim to alleviate the signs and symptoms of the disease and to slow its progression. Despite prevention has a key role to avoid or at least delay the occurrence of OA, in some cases a surgical procedure, such as total knee arthroplasty (TKA), is necessary to decrease pain and improve knee function [25]. The three main prosthesis components, which are the femoral component, the tibial tray and the tibial component, can be visualized in Figure 2.18.

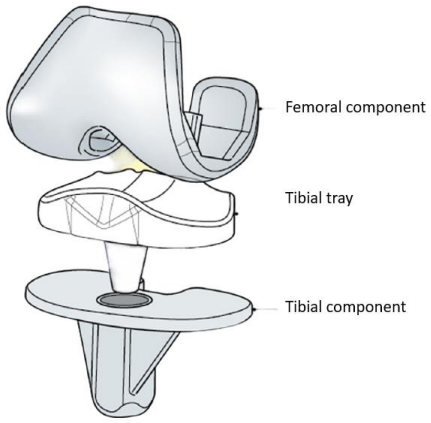

Figure 2.18 Prosthesis components.

Nonetheless, some patients complain about poor results after surgery or the implant fails and thus revision surgery is required. It has been found that one of the failure causes is related to polyethylene wear and consequently aseptic loosening that leads to early revision [26]. This observation can be attributed to the components misalignment which provoke an uneven distribution of the stress onto the tibial tray.

3 State of the art

The needs of understanding the kinematics and the loads effects onto the knee during daily activities has been led to investigate the biomechanical behaviour of the knee joint using numerical methods. In this context, the FEA has made its way. It represents a numerical process to solve engineering questions and mathematical physics. To solve them, it subdivides a large problem into smaller simpler parts that are called finite elements. The simple equations that model these finite elements are then assembled into a larger system of equations to represent the entire problem. The main advantage of using FEA is that it is cost-effective, since running an analysis by means of this computational method is cheaper than performing a physical experiment. Modern finite element models usually are based on magnetic resonance imaging (MRI) or computed tomography (CT) scans and provide a high degree of anatomical realism [27]. Specifically, FEA has been recognized significantly and widely used in the field of knee prosthesis to perform numerical simulations under different types of configurations and loadings. Indeed, the use of the method in these terms, together with orthopaedics observations, has led to a better understanding of the role of knee misalignment in TKA components. FEA is in fact a useful tool for the prediction and measurement of local parameters such as internal stress, strain, and displacement or to detect abnormal forces generation which can be the cause of TKA failure and in some cases knee pain, thus affecting the joint kinematics. One of the causes is related to axial knee misalignment which is considered one of the biomechanical key factors that brings to knee pain and an early deterioration of the polyethylene insert [2]. From these observations and studies, it comes the role of knee misalignment also in healthy knee. In fact, the internal rotation of the tibia with respect to the femur is correlated with the progression of knee OA [10]. Several studies have been conducted on healthy knees using FEA.

Despite this, still nowadays none of them considered the comparison among different femoral-tibial torsion configurations to better understand the role of knee misalignment also in healthy knees.

In this scenario, the accurate research in the literature of FEA models have been divided into two different sections:

- In Section 4.1 there are studies that used FEA to investigate normal knee models in different conditions.
- In Section 4.2 there are those works that study the effect of components misalignment in FEA 3D TKA models.

3.1 FEA 3D models to study normal knee biomechanics

Devaraj et al. [28] performed a 3D reconstruction of a healthy knee joint from an MRI scan in order to determine the stresses in the knee joint. The 3D surface meshed models generated by Mimics contain a large number of triangles with high aspect ratios. The model was exported in ANSYS Workbench v16.2. The bone, menisci, cartilage and ligaments were assumed to be linearly elastic and isotropic. The material properties of each knee joint part are specified in Table 1.

Table 1 Material properties of various parts of the knee joint [28].

Component	Young modulus (E) [MPa]	Poisson's ratio
Bones	17'400	0.3
Ligaments	60	0.3
Cartilage	12	0.45
Meniscus	59	0.49

The bonded contact was set to represent the contact between bone-cartilage, bone-ligament, and medial collateral ligament-medial meniscus. No separation contact was defined between the femoral cartilage-tibial cartilages, cartilages-menisci and femoral cartilage-patellar cartilage. Flexion/extension and varus/valgus rotations were constrained for the femur to analyse the knee joint in full extension. The tibia and fibula were fixed at the lower surfaces.

A vertical compressive force of 1150 N was applied on the top of the femur, representing the force of the gait cycle in a full extension position. The boundary conditions can be appreciated in Figure 3.1.

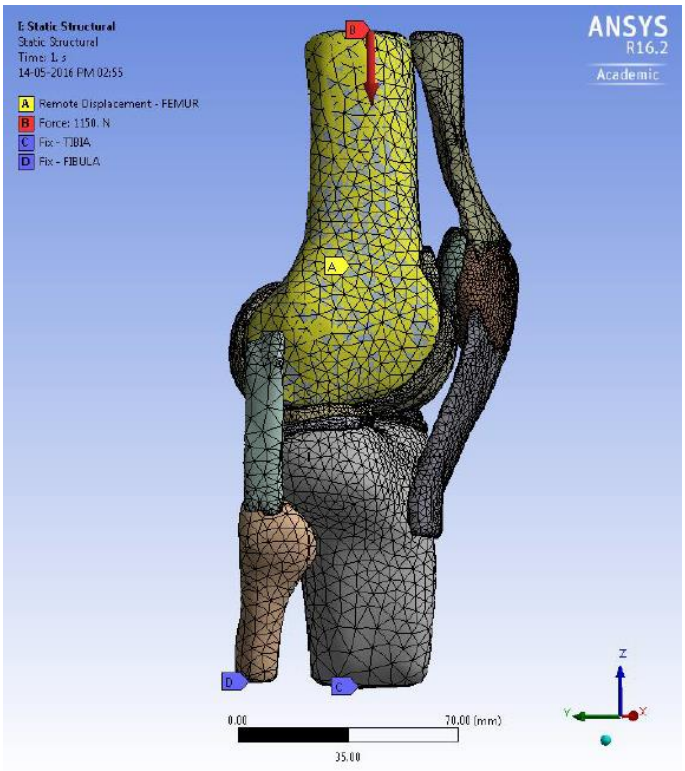

Figure 3.1 Boundary conditions of the model [28]

The menisci stress can be found in Figure 3.2, on the left it is represented the lateral meniscus and, on the right, the medial one.

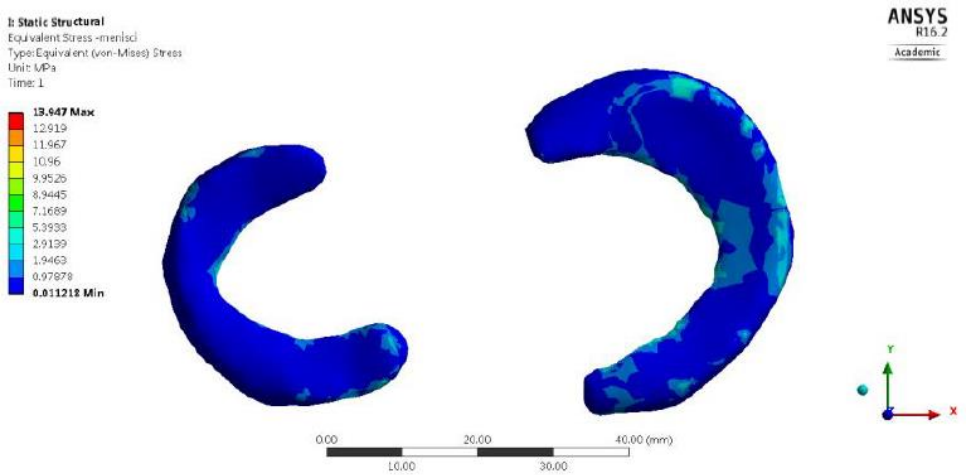

Figure 3.2 Menisci von-Mises stress [28].

The magnitudes of Von Mises stress of 5.43 MPa was higher on the medial meniscus compared to the lateral meniscus with 3 MPa. Thus, it was concluded that medial meniscus is more likely to rupture.

Abidin et al. [12] tried to provide a more precise human joint representation using FEA. In particular, in the development of the virtual model an accurate attention for the segmentation of the cortical and cancellous part of the bones was made as can be seen from Figure 3.3.

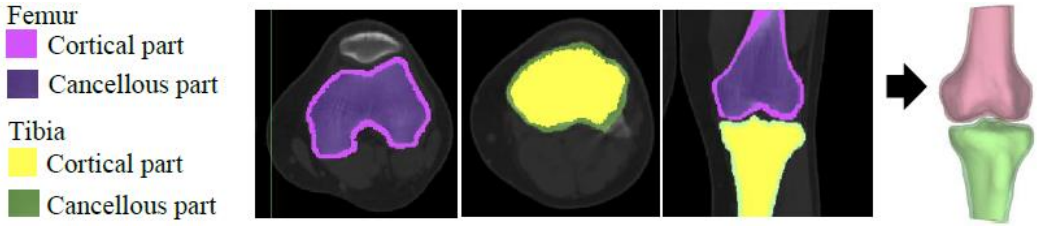

Figure 3.3 Segmentation of cortical and cancellous bone of the femur and tibia [12].

The cartilages are considered to be linear elastic and isotropic. Linear spring elements were used to model four ligaments at knee joint: ACL, PCL, MCL and LCL, by referring to anatomical attachment sites. The knee joint was set into two degrees of knee flexion which are at 0° and 30° of flexion. The considered mechanical properties of bones and cartilages and stiffness coefficient of the ligaments are listed in Table 2.

Table 2 Mechanical properties and stiffness coefficient.

Tissue	K (N/mm)	E (MPa)	Poisson's ratio
Cortical bone	-	16200	0.36
Cancellous bone	-	389	0.3
Articular cartilages	-	10	0.4
ACL	75	-	-
PCL	75	-	-
LCL	20	-	-
MCL	70	-	-

In Figure 3.4 and Figure 3.5 the Peak Von Mises Stresses (VMS) on the articular cartilages at different loads configurations and at 0° and 30°, respectively, are represented.

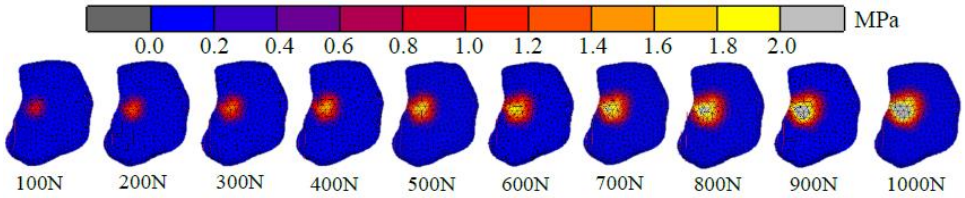

Figure 3.4 Contour plot of Peak VMS at articular cartilages [12].

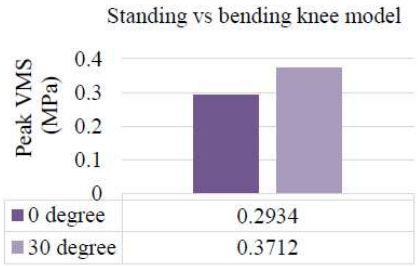

Figure 3.5 Peak VMS at articular cartilages on knee joint at 0° and 30° knee flexion [12].

From the presented figures, the value of peak VMS at knee joint increases with the increment of compression loading force and it is also proven that the increase of knee flexion will decrease the contact area thus increasing the contact pressure at knee joint.

Another interesting paper is the one of Andriacchi et al. [8], in which the rotational changes at the knee after ACL injury were investigated. In particular, FEA was used to examine the hypothesis that a 5° internal tibial rotation after ACL injury accelerates cartilage thinning with respect to a healthy knee during walking (Figure 3.6).

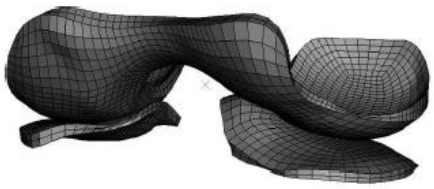

Figure 3.6 3D FE mesh of femoral and tibial cartilage [8].

To compare the differences in cartilage thinning between knees in healthy and ACL-deficient patients, the thinning simulation analysis was conducted for a normal and a rotated (ACL-deficient) knee. The alignment of the ACL-deficient knee was modelled by rotating the tibia 5° internally from the normal knee. The cartilage was assumed as linear elastic, isotropic body with a Young's modulus of 6 MPa and Poisson's ratio of 0.47. The subchondral bone was modelled as rigid.

A coefficient of friction at the articular surface of 0.1 was set to simulate the condition of initial cartilage break down. Furthermore, the applied kinematic and load measurements were derived from a defined study of subjects with ACL-deficient and healthy knees. The results of the considered study are shown in Figure 3.7.

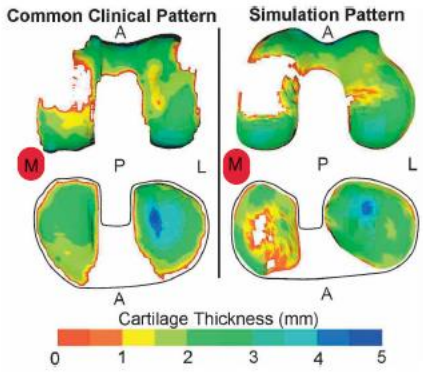

Figure 3.7 A comparison of a cartilage thickness map of a patient with end-stage knee OA with the predicted thinning regions [8].

On the tibia, the degeneration was almost entirely in the anterior portion of the medial side. The model also predicted a greater rate of cartilage loss in the medial compartment relative to the lateral one. In addition, the rate of loss on the medial tibial cartilage increased with time as the cartilage loss moved to the medial boundary of the medial compartment. Thus, the internal rotation associated with the ACL-deficient knee shifted the load bearing to thinner regions of cartilage, resulting in increased stresses in the cartilage and accelerated the its loss. This explains the increased incidence of medial compartment knee OA after ACL injury and provoked by the consequent tibial internal rotation.

3.2 FEA 3D TKA models with misalignment

Liau et al. [4] have used the FEA, performed in ABAQUS, to investigate the effects of different misalignments on stresses in tibial polyethylene component of total knee prostheses. In particular, 3D FE models of the tibiofemoral joint of knee prostheses for three different designs were built. This work investigated the neutral position together with other three malalignment conditions: medial translation (0.25, 0.5 and 1.0 mm), internal rotation (1°, 3° and 5°), and varus tilt (1°, 3° and 5°) of the femoral component with respect to the tibial component (Figure 3.8).

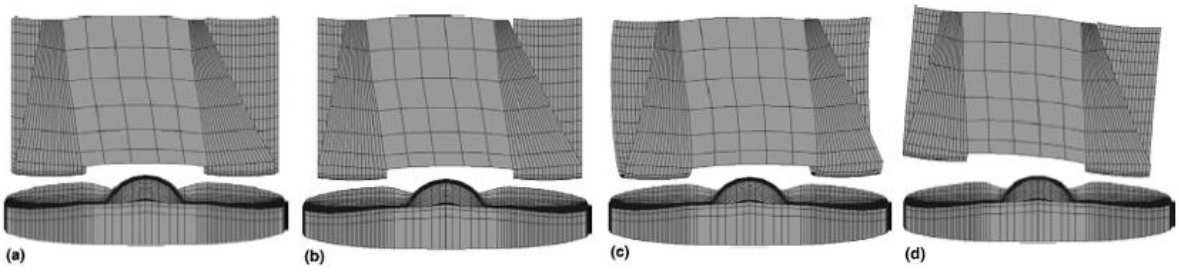

Figure 3.8 Prosthesis conditions: neutral (a), maltranslation (b), malrotation (c), varus tilt (d) [4].

The bearing surface of femoral component was modelled with rigid body elements since the elastic modulus of the femoral component was much larger than the ultra-high molecular weight polyethylene (UHMWPE) tibial component. A total of 11,232 eight-node solid block elements were used to model the tibial component. The UHMWPE tibial component was assumed as an elastic-plastic material.

Moreover, the elastic modulus was 1016 MPa, the Poisson's ratio was 0.46 and the yield stress was 14.07 MPa. About the boundary condition, the fixed support was specified on the base of the tibial component. The femoral component instead was constrained to move vertically only. Then a compression load equal to 3000 N, usually used to evaluate the contact characteristics in tibiofemoral joint of knee prostheses, was applied to the tibiofemoral joint at 0° of flexion. The contact pairs between the polyethylene insert and femoral component was assumed as frictionless. From the results can be highlighted that the malrotation of the femoral component just slightly increase the risk of polyethylene wear in tibial component. However, in this study, only a vertical compression load was applied to the tibiofemoral joint of knee prostheses at 0° of flexion. The knee kinematics and the cyclic repetition of load were also important factors, which were not considered in [4]. Moreover, here just small malrotation values were considered.

A similar study was conducted in [29]. The aim was the evaluation by means of FEA of tibial baseplate malpositioning effects in the same knee during the squat. In particular, 3° and 6° of internal rotation of the tibial baseplate was considered. For the simulation, an established weight-bearing finite element model (FEM) for TKA previously described by Woiczinski et al. was used. The ligaments were modelled as linear spring elements in bundle technique. In particular, one spring was used for the LCL, two for the PCL (PCLa for the anterior and PCLp for the posterior bundle) and three for the MCL (MCLa, MCLo and MCLs that stands for anterior, oblique and superficial bundle), as shown in Figure 3.9.

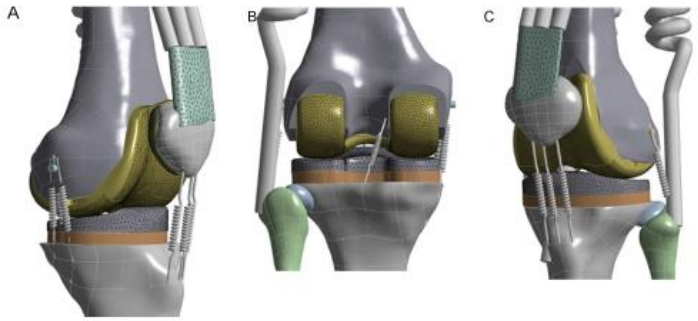

Figure 3.9 Finite element model with ligaments as springs: medial view (A), posterior view (B) and anterolateral view (C) [29].

Several muscles forces were considered in the simulation and in order to guarantee the correct direction of the force during the squat they were represented by spring elements. For what concerns the frictional coefficient, it was set at 0.02 and at 0.05 for the patellofemoral joint and the tibiofemoral joint, respectively. From the results, the load augment with the increase of flexion angle. Furthermore, it seems that the internal rotation had only a small influence in the ligament tensions. This seems to be in contrast with the findings of [30] in which the considered model (Figure 3.10) revealed that the internal rotation provokes a significant increase in MCL tension.

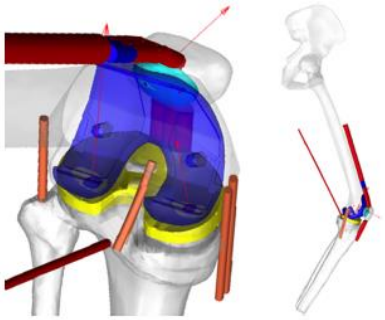

Figure 3.10 Ligaments attachment points and boundary conditions of the model [30].

This difference could be due to different malrotation angles. In fact, in [30] the tibial rotational alignment was set to 15° internal rotation, higher value with respect to those used in [29]. Figure 3.11 reports the negative effect of the internal misalignment of the insert, since a greater contact stress occurs with respect to the neutral alignment.

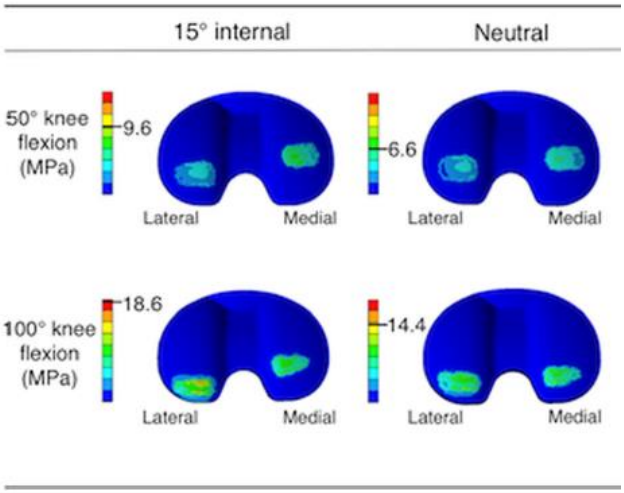

Figure 3.11 Tibiofemoral peak contact stresses at the component interfaces with malrotation at 50° and 100° of flexion [30].

The study of Osano et al. [6] also investigated the effect of malrotation of tibial component in TKA model, during high flexion. A posterior-stabilized total knee prosthesis, Scorpio NRG (Stryker Co., Kalamazoo, USA), was used for the analysis. The tibial insert made of ultra-high-molecular-weight polyethylene (UHMWPE) was assumed to be elastic-plastic material. Femoral and tibial components made of Co-Cr alloy were assumed to be rigid for reducing computational complexity. A coefficient of friction of articular surface was set to be 0.04. Four non-linear springs were attached to tibial component in order to represent soft tissues around the knee. The boundary conditions are shown in Figure 3.12.

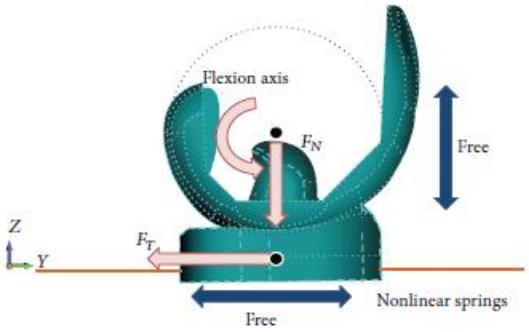

Figure 3.12 Boundary conditions of the study [6].

The femoral component was allowed to translate in the vertical direction and rotate about a transverse axis to simulate flexion and extension. The tibial component was allowed to translate in the AP direction and rotate about a vertical axis located in the center of tibial condyles to simulate internal and external rotation. Vertical load was applied to the femoral component which rotated from 0◦ to 135◦ of flexion while horizontal load along the AP direction was applied to the tibial component which internally rotated from 0◦ to 15◦ of rotation during knee flexion. Figure 3.13 and Figure 3.14 show the stress on the tibial insert in the normal (NRM) configuration and in the one internally rotated of 15° (IR).

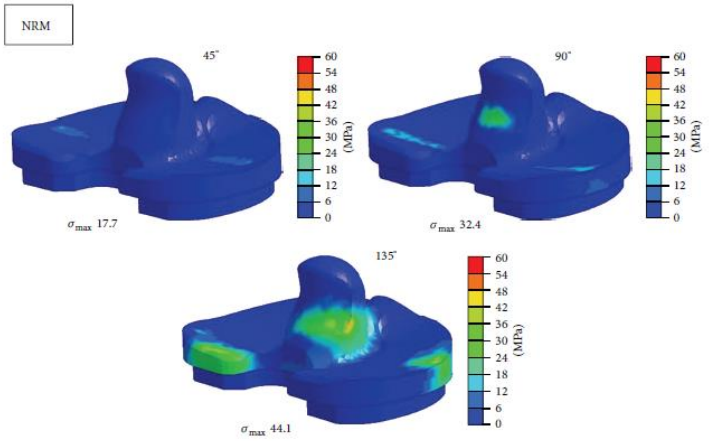

Figure 3.13 Maximum equivalent stress distribution in tibial insert at each position at the flexion angle of 45 °, 90 °, and 135 °. σmax= maximum equivalent stress. NRM = normal [6].

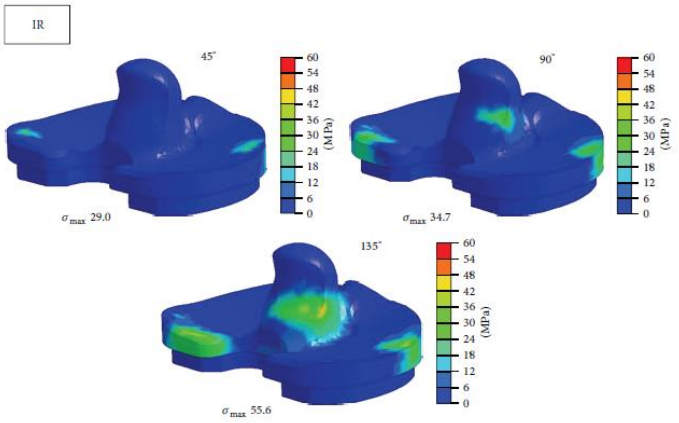

Figure 3.14 Maximum equivalent stress distribution in tibial insert at each position at the flexion angle of 45 °, 90 °, and 135 °. σmax= maximum equivalent stress. IR = internal rotation [6].

Thus, the results of this study revealed that malrotation that presents an excessive internal rotation increase the stress on tibial insert significantly. Therefore, internal rotation of tibial component should be avoided.

In summary, after an accurate research, in literature there were studies related to:

- FEA on healthy knee models without prosthesis in the extension position and during flexion;
- FEA on injured knee model without prosthesis with a tibial internal rotation;
- FEA on TKA knee models in which it was performed a comparison between normal and tibial component internal rotation configurations.

Accordingly, no studies related to the comparison of healthy knee models characterized by a tibial internal rotation and a normal knee alignment have been conducted. For this reason, this work aims to develop and compare the effects of these two different femoral-tibial torsion configurations. In particular, the aim is to confirm the orthopaedist findings, according to which:

- Stress changes are in the medial part of the knee;
- Tibial internal rotation in the range of (-16°, -9.1°; OA subject [10]) provokes higher stresses than a more external femoral-tibial torsion configuration (normal configuration) in the range of (-3°, 0.9°; non-arthritic subject [10]). This will confirm the correlation between tibial internal rotation and OA development.

4 Materials and methods

This section will present the workflow of the current study divided in two parts. The first part will describe the models reconstruction procedure to obtain two different 3D knee models with a femoral-tibial torsion of -11° and 0° and they will be referred as internal rotation model and external rotation model respectively. Then, in the second part a detailed description of the FEA settings can be found.

All the followed steps have been summarized in Figure 4.1.

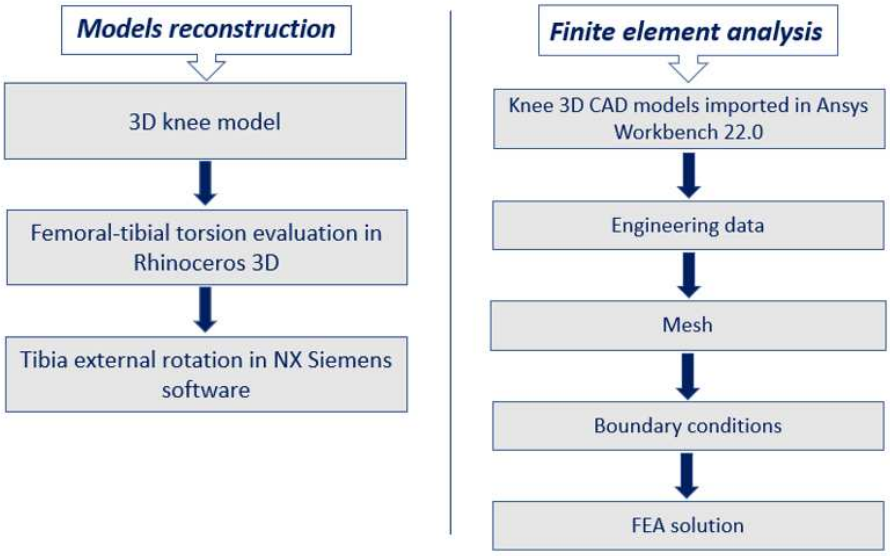

Figure 4.1 Workflow of the study.

4.1 Models reconstruction

In order to reconstruct the two knee models, the starting point has been a predefined standardized knee geometry designed on CINEMA 4D 18 software. It is characterized by 10000 polygons, 1000000 vertices and it is in the flexion position as can be appreciated in Figure 4.2.

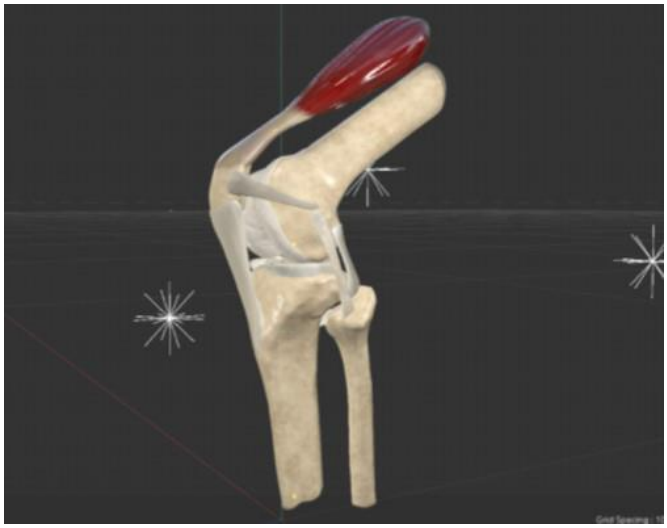

Figure 4.2 Standardized knee geometry in Cinema 4D 18 software.

Specifically, the model is composed of the following structures: femur, tibia, patella, fibula, femoral cartilage, medial and lateral menisci, QT, PT, MCL, LCL, PFL, LPFL and MPFL. This standard model was modified by a previous study in order to obtain a knee in the extended position and the MCL, PFL, tendons, and menisci were remodelled.

Then, this extended knee model was imported in Rhinoceros 3D software in order to calculate the femoral-tibial torsion. In particular, just the femur, the femur cartilage, the lateral meniscus, the medial meniscus and the tibia have been considered for the current study. The transepicondylar surgical axis (TEA) and the tangent to the posterior surface of the tibia (PTT) have been identified under the examination of a specialist orthopaedic surgeon (Figure 4.3).

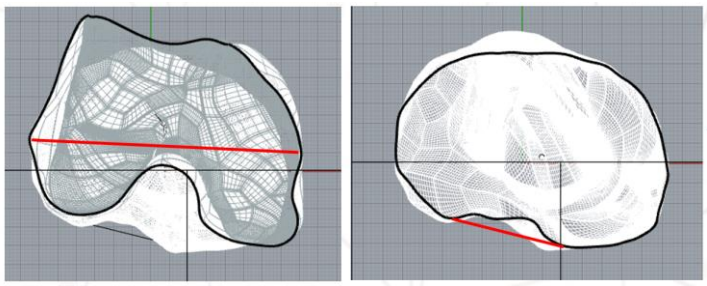

Figure 4.3 Identified transepicondylar surgical axis (TEA) (left) and the tangent to the posterior surface of the tibia (PTT) (right) in the internal rotation knee model.

It has been found that the angle formed by the previous described axes is about -11° and since this study aims to develop and analyse a 3D knee model that present a femoral-tibial torsion of -11°, the starting model has been used to study the effects of tibia internal rotation (Figure 4.4).

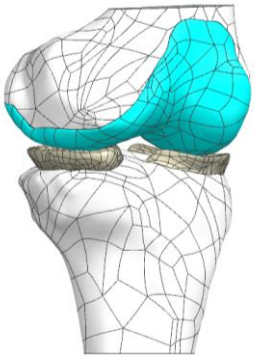

Figure 4.4 3D knee model: tibial internal rotation model.

Finally, the aforementioned knee geometry has been imported in NX Siemens software to perform a tibia external rotation of 11° necessary to obtain the second model. As confirmed from the detection of the TEA and PTT axes the femoral-tibial torsion was equal to 0° (Figure 4.5).

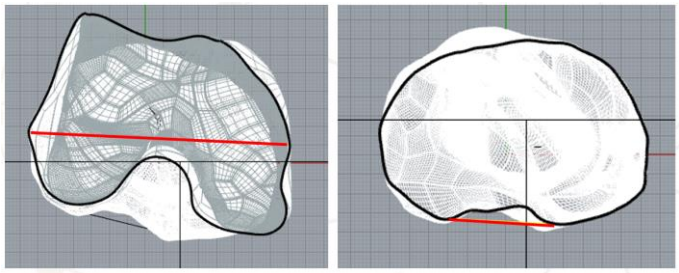

Figure 4.5 Identified transepicondylar surgical axis (TEA) (left) and the tangent to the posterior surface of the tibia (PTT) (right) in the external rotation knee model.

Moreover, a tibia and menisci translation of 2 mm in the antero-direction was applied in order to obtain a better match between the femur and menisci profiles with an even distance between them. Thus, the external rotation model refers to this latter described geometry (Figure 4.5).

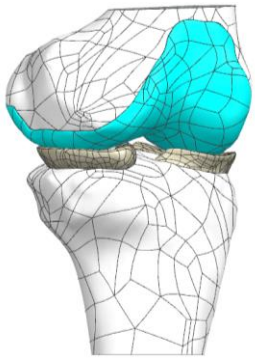

Figure 4.6 3D knee model: tibial external rotation model.

At last, Boolean operations were performed on both models to ensure that no bodies intersection existed.

4.2 Finite element analysis

The final step of the present study consists of two Static Structural FEA performed by means of Ansys Workbench 2022 R2. The 3D knee models were imported in Ansys Design Modeler to generate the five solid bodies. At each model was applied the same setting in order to obtain a reliable comparison between the results.

The materials have been considered as isotropic, homogeneous, and linearly elastic according to [31]. This assumption provides a good approximation of the mechanical properties to obtain a qualitative comparison among different configurations [32]. In Table 3 can be found the setting of the Engineering Data, thus the list of the considered elastic properties, in particular the Young modulus and the Poisson's ratio [33][34][35].

Table 3 Material properties used in this study.

Component	Young modulus	Poisson's ratio
Femur	17'000	0.3
Femur cartilage	5	0.45
Tibia	15'000	0.3
Menisci	59	0.49
ACL	123	0.4
PCL	168	0.4
LCL	280	0.4
MCL	224	0.4

Three bonded contacts have been defined between femur-femur cartilage, tibia-lateral meniscus and tibia-medial meniscus allowing no sliding and no separations between the target and the contact. Additionally, six frictionless contacts were set between femur cartilage-lateral meniscus, femoral cartilage-medial meniscus, tibia-femur cartilage, femur-lateral meniscus, femur-medial meniscus and tibia-femur allowing free sliding on the target surface due to the friction coefficient equal to zero and also the translation in the normal direction [36]. This last choice was made due to the very poor friction coefficient that characterize the roll-back movement, as stated in [21].

All the contacts have been listed in Table 4.

Table 4 Contact pairs.

Type	Contact body	Target body
Bonded	Femur	Femur cartilage
Bonded	Tibia	Lateral meniscus
Bonded	Tibia	Medial meniscus
Frictionless	Femur cartilage	Lateral meniscus
Frictionless	Femur cartilage	Medial meniscus
Frictionless	Tibia	Femur cartilage
Frictionless	Femur	Lateral meniscus
Frictionless	Femur	Medial meniscus
Frictionless	Tibia	Femur

Due to the large number of elements and nodes and for the presence of nonlinear contacts, it has been used the Auto Time Stepping to divide the analysis into smaller substeps, in particular the Initial Substeps was set at 10 while the Minimum and Maximum Substeps were set at 5 and 2000 respectively.

Moreover, the NEQIT command has been set to 200 to guarantee the convergence of the simulation.

The knee ligaments are the most critical parts to determine due to the complexity of their simulation. In literature, a wide range of different approaches have been found to try to easily represent their biomechanics [27]. Among them, the beams which consists in a line element representation with a linear elastic isotropic behaviour have been considered, as suggested in [31]. In particular, four different knee ligaments have been represented in this 1D configuration and they were placed following the knee anatomy. Thus, the ACL and PCL were cross positioned in the centre part of the knee while the LCL and MCL were placed respectively in the lateral and medial part of the knee. Figure 4.6 shows the configurated beams and as can be seen the LCL was attached to the tibia since the fibula geometry was not available while the MCL was characterized by two beams according to [32]. Furthermore, at each ligament modelled as a beam was assigned the elastic properties according to [37] that were inserted in Table 3. They were also characterized by a circular cross-section, with a radius of 0.3 mm for the cruciate ligaments and 0.2 mm for the collateral ones.

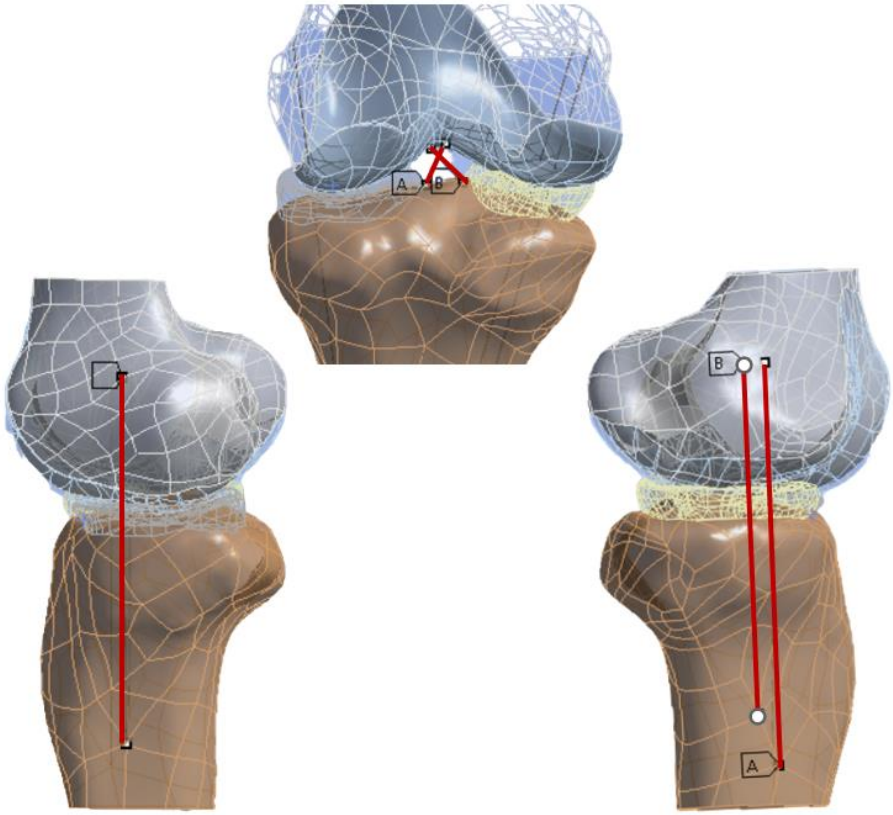

Figure 4.7 Ligaments represented as beam elements: LCL (left), ACL (A)(middle), PCL (B)(middle) and MCL (A-B)(right).

Since this study aims to analyse the models during the flexion, four boundary conditions have been imposed. The first condition has fixed the tibia at its distal end to avoid movements; in the second condition a force of -200N has been applied to the femur to simulate the load on the knee as done in [38]. As third condition, a Remote Displacement along the X-axis was applied on the top face of the femur to bring the knee in the flexion position. In particular, the simulation was set at five different substeps, each characterized by a different flexion angle with a maximum value of 40° (0°, 10°, 20°, 30° and 40°). Finally, the fourth and last condition was related to the Displacement of the femur lateral and medial parts. More in detail, two different displacements were imposed according to [39]. Despite these values refers to measurements conducted in subjects that undergo bi-cruciate-stabilized total knee arthroplasty (BCS-TKA), they are suitable for this study since [40] and [41] prove that BCS-TKA can reproduce physiological sagittal plane kinematics. Moreover, the considered values are similar to those found in [42] that conducted the research on normal knees. The application points of the lateral and medial displacement are shown in Figure 4.7 and the information about these last two conditions is summarized in Table 5.

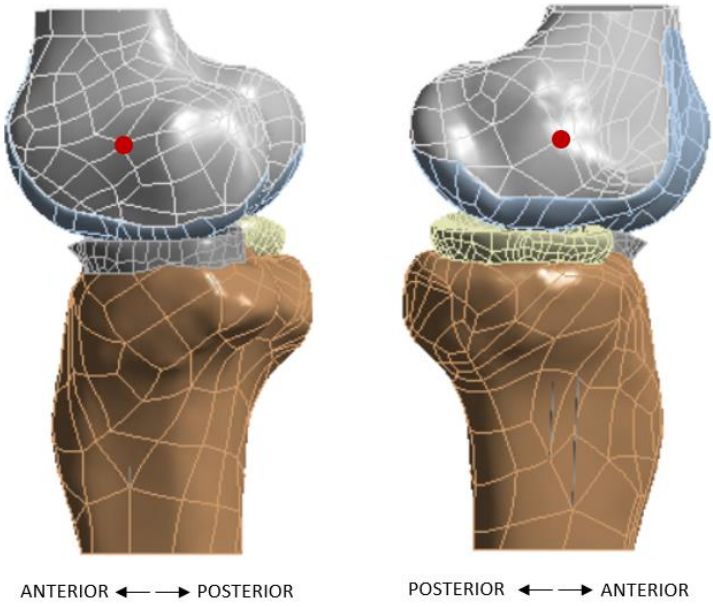

Figure 4.8 Point of application of the lateral displacement (left) and medial displacement (right).

Table 5 Lateral and medial displacement applied to the femur.

Substep	Remote Displacement	Lateral Displacement (mm) + Anterior direction - Posterior direction	Medial Displacement (mm) + Anterior direction - Posterior direction
1	0°	0	1
2	10°	-6	-2
3	20°	-8	-3.2
4	30°	-8.1	-3
5	40°	-8.1	-2.7

All the four boundary conditions are shown in Figure 4.8.

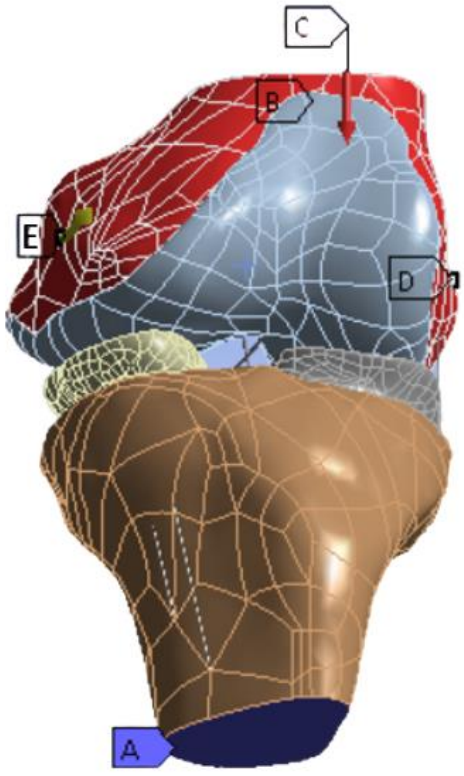

Figure 4.9 Four boundary conditions: Fixed Support (A), Remote Displacement (B), applied Force (C), lateral and medial Displacements (D-E).

After the definition of the contacts and the boundary conditions, the mesh was generated choosing the most suitable mesh element. Of course, the use of smaller elements allows the achievement of a more accurate discretization with a better fit of the model original shape and the improvement of the outputs accuracy. On the other side, the increment of the number of nodes and hence the number of equations leads to an increase in the computational time. For this reason, a trade-off between accuracy and computational time has been considered. The geometries have been all meshed with linear tetrahedral elements as can be appreciated in Figure 4.9 and the total number of nodes and elements for each knee components have been listed in Table 6**.**

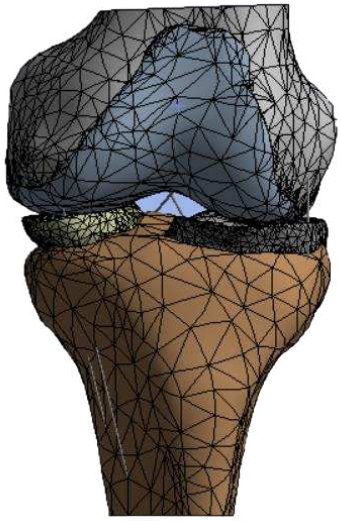

Figure 4.10 Mesh representation of the knee model.

Table 6 Nodes and elements of the 3D TKA model.

Structure	Nodes	Elements
Femur	10589	6162
Femur cartilage	7097	3331
Tibia	2889	1552
Lateral meniscus	4598	2263
Medial meniscus	4626	2449

5 Results

This section summarizes all the results coming from the static structural analysis. In particular, the knee kinematics, the von-Mises stresses of the menisci and the von-Mises stresses of the tibia have been highlighted.

5.1 Knee kinematics

The flexion of the knee at each considered substep for the internal and external rotation models are illustrated in Figure 5.1 and Figure 5.2 respectively.

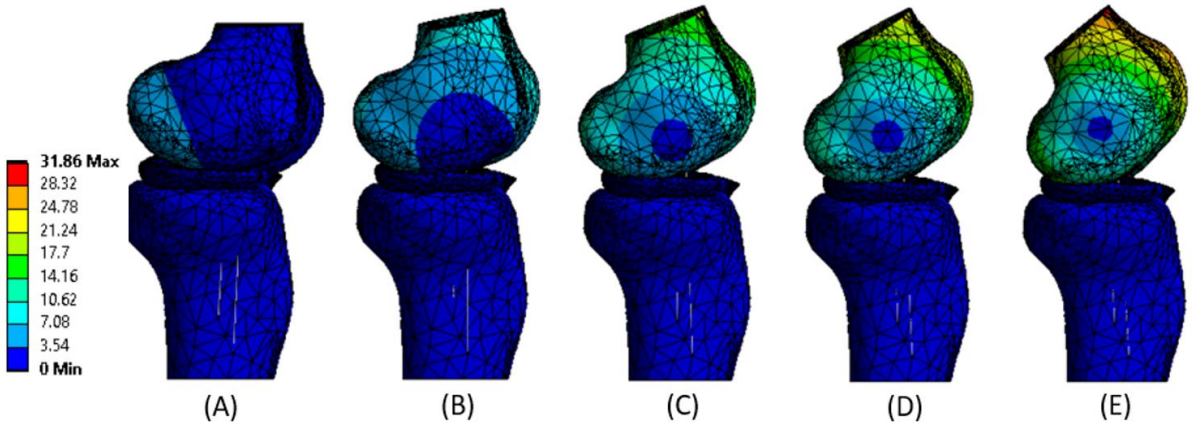

Figure 5.1 Knee flexion of the internal rotation model at: 0°, 10°, 20°, 30° and 40° (A-E): Total Deformation representations.

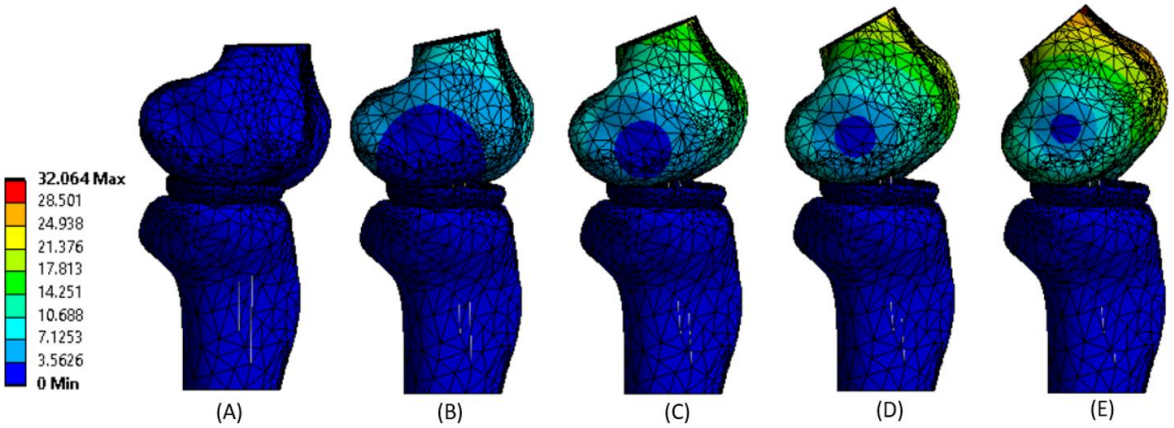

Figure 5.2 Knee flexion of the external rotation model at: 0°, 10°, 20°, 30° and 40° (A-E): Total Deformation representations.

Table 7 lists the flexion angles and the femur external rotation angles measured in the Remote Point applied to the femur, in both models. These values are useful to verify if the model performed the correct movement imposed by the boundary conditions.

Table 7 Measured rotations in the femur Remote Point.

	INTERNAL rotation model	EXTERNAL rotation model
FLEXION	40°	40°
FEMUR EXTERNAL ROTATION	3.4°	4.6°

5.2 Von-Mises stresses of menisci

Figure 5.3 summarizes the Maximum and Average von-Mises stresses of the menisci obtained at each considered flexion angles, for both the models.

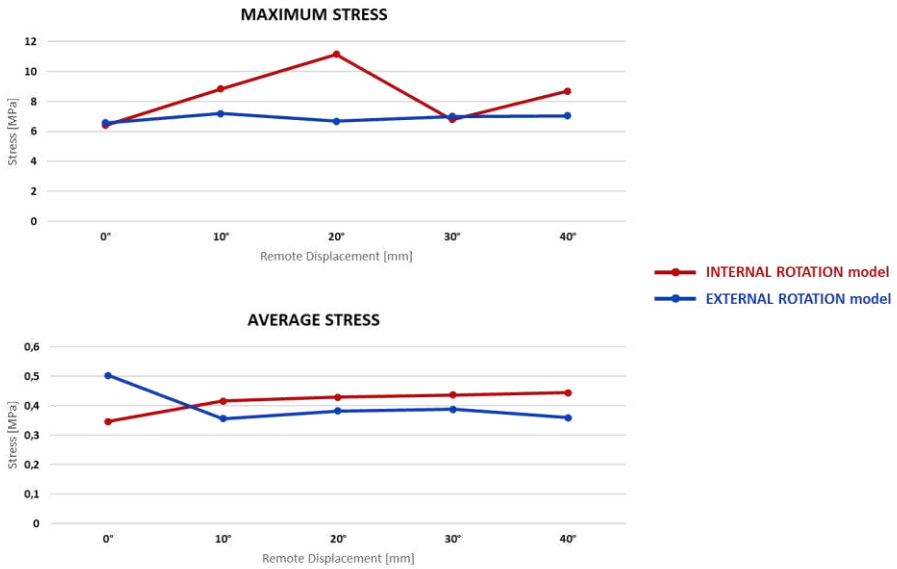

Figure 5.3 Maximum and average menisci stresses of both models.

Figure 5.4-5.8 show the graphical representation of the menisci von-Mises stresses of the internal and external rotation model. In particular, the lateral meniscus is on the left while the medial one is on the right.

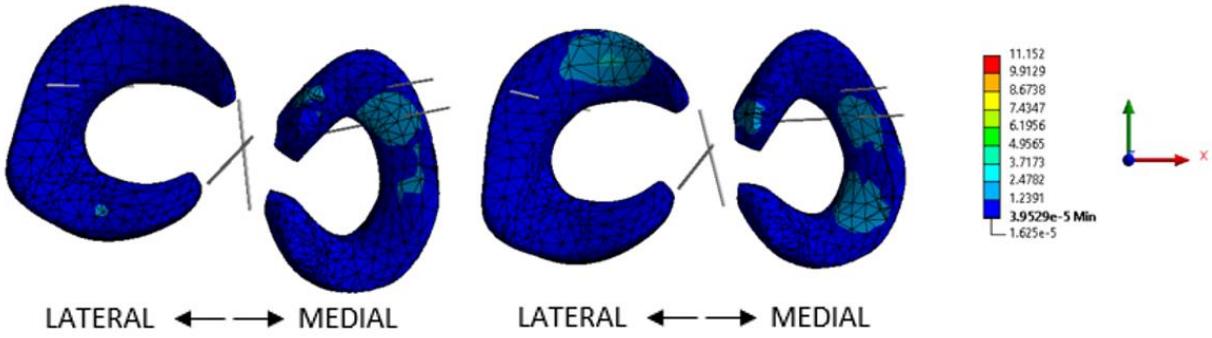

Figure 5.4 Menisci stresses of the internal rotation (left) and external rotation (right) models at 0° of flexion.

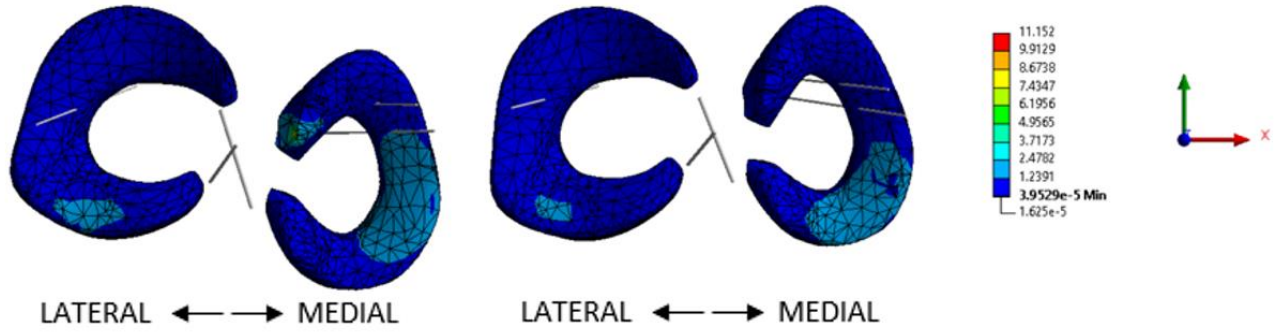

Figure 5.5 Menisci stresses of the internal rotation (left) and external rotation (right) models at 10° of flexion.

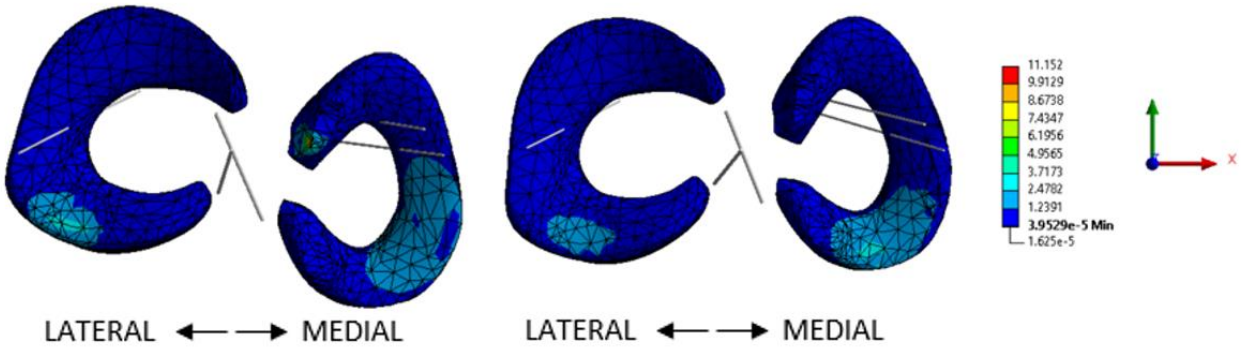

Figure 5.6 Menisci stresses of the internal rotation (left) and external rotation (right) models at 20° of flexion.

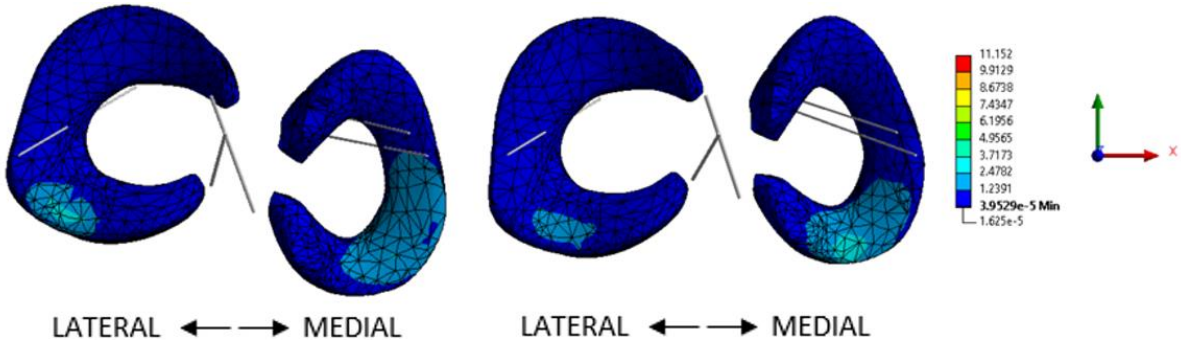

Figure 5.7 Menisci stresses of the internal rotation (left) and external rotation (right) models at 30° of flexion.

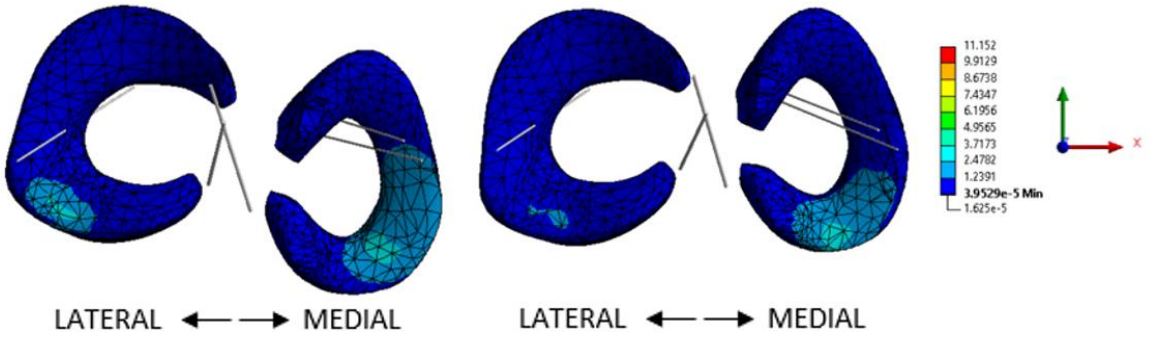

Figure 5.8 Menisci stresses of the internal rotation (left) and external rotation (right) models at 40° of flexion.

5.3 Von-Mises stresses of tibia

Figure 5.9 summarizes the Maximum and Average von-Mises stress of the tibia obtained at each considered flexion angles, for both the models.

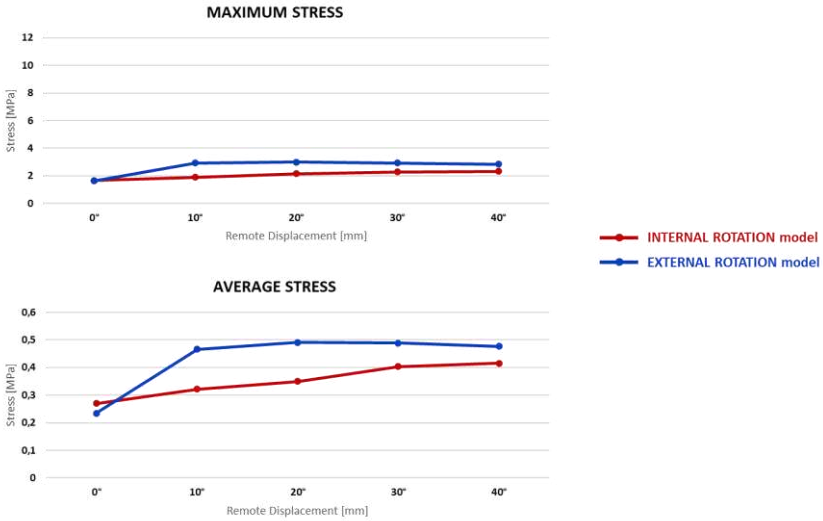

Figure 5.9 Maximum and average tibia stresses of both models.

Figure 5.10-5.14 represent the graphical representation of the tibia von-Mises stresses of the internal and external rotation models. In particular, it is represented the top view of the tibia to highlight the stresses between the femoral-tibial interface.

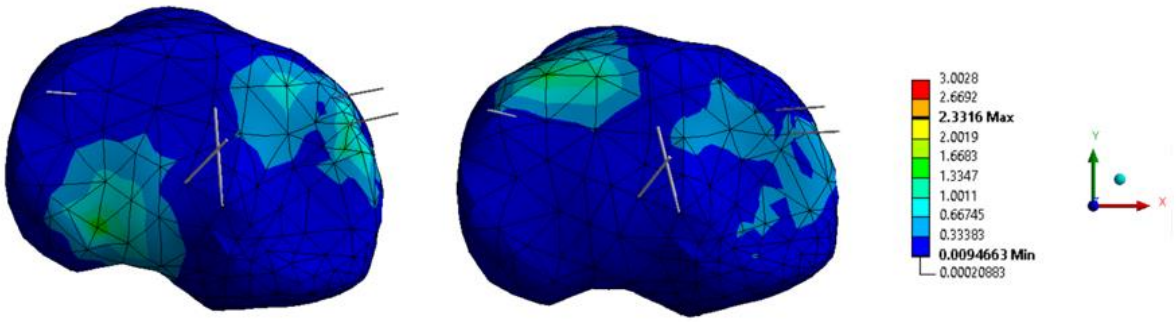

Figure 5.10 Tibia stresses of the internal rotation (left) and external rotation (right) models at 0° of flexion.

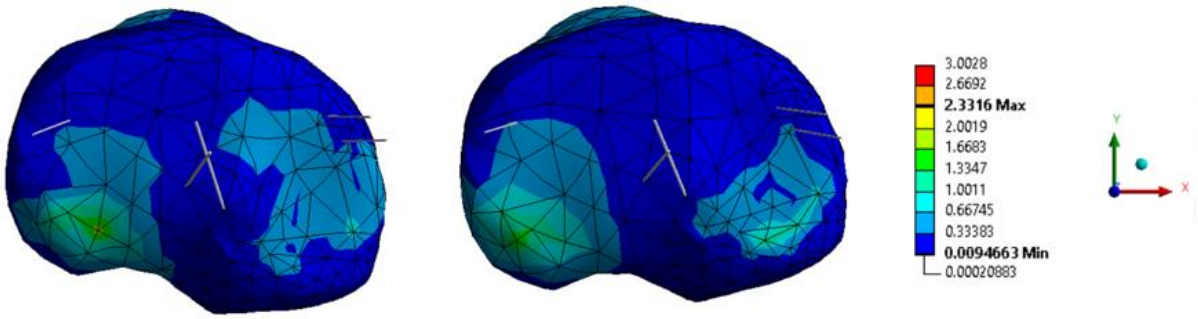

Figure 5.11 Tibia stresses of the internal rotation (left) and external rotation (right) models at 10° of flexion.

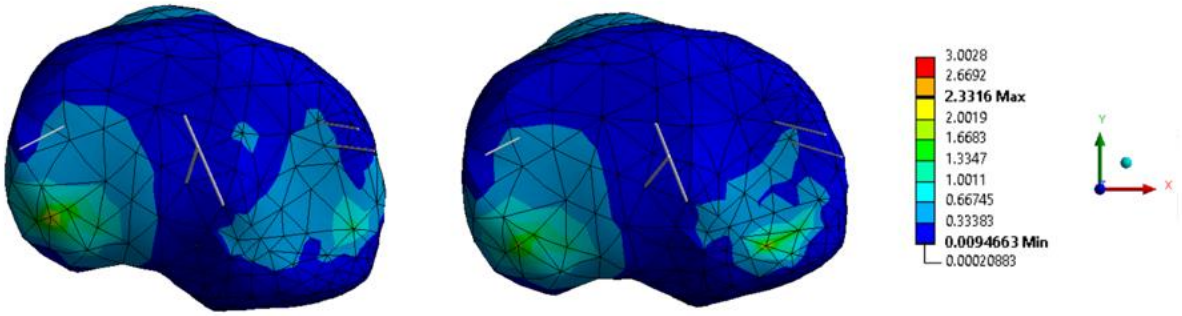

Figure 5.12 Tibia stresses of the internal rotation (left) and external rotation (right) models at 20° of flexion.

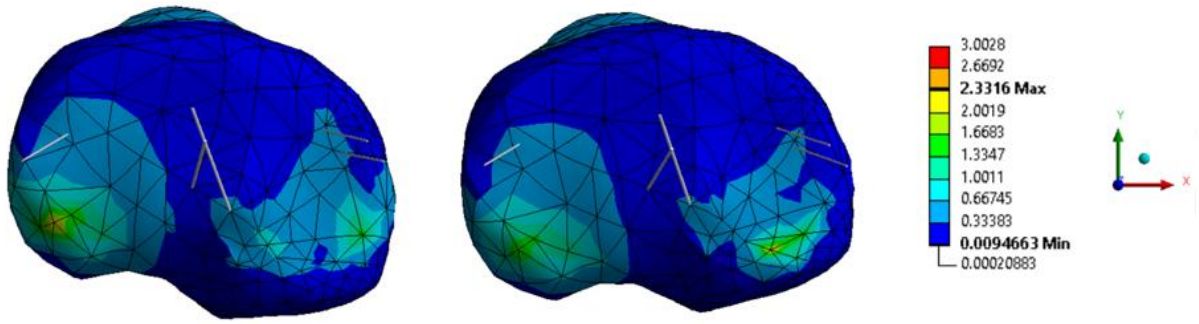

Figure 5.13 Tibia stresses of the internal rotation (left) and external rotation (right) models at 30° of flexion.

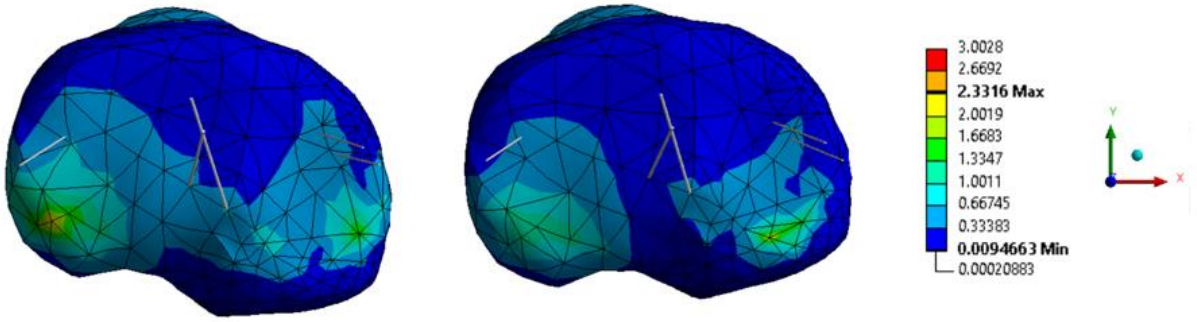

Figure 5.14 Tibia stresses of the internal rotation (left) and external rotation (right) models at 40° of flexion.

It is also important to compare the stresses obtained in the medial part of both the models at 40° with the wear on tibial cartilage of a real knee. This comparison can be found in Figure 5.15.

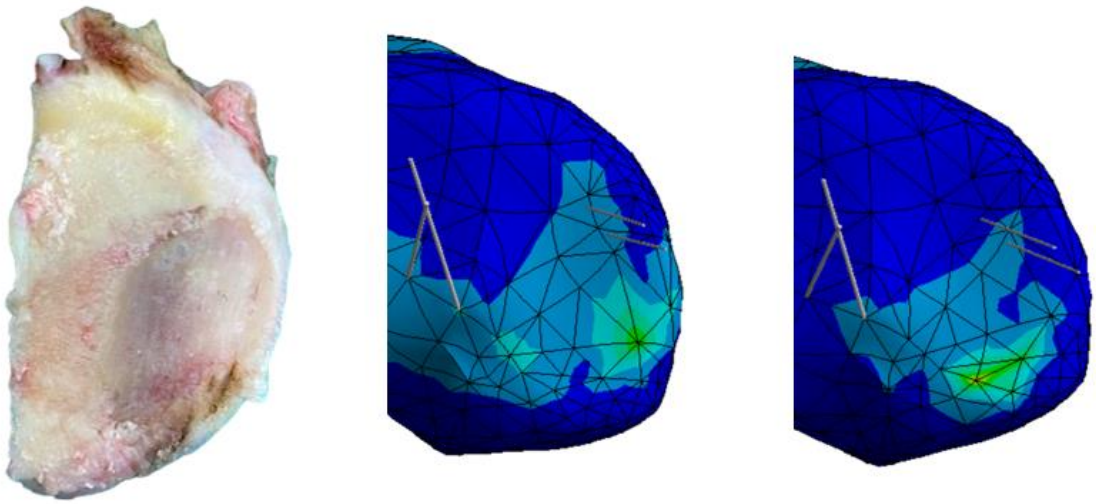

Figure 5.15 Comparison between the wear on tibial cartilage of a real knee (left), the tibia stress of the internal rotation model at 40° (middle) and the tibia stress of the external rotation model at 40° (right).

6 Discussion

The knee represents the biggest and most complex human joint and still nowadays many aspects related to the maintenance of knee stability need to be investigated. The articular cartilage wear leads to the OA development and thus requires a proper treatment to restore the knee functionality. Indeed, TKA is one of the most successful surgeries performed in orthopaedics. Despite this, patient-reported outcomes have shown dissatisfaction after the surgical procedure, also complaining about knee pain [25]. One of the causes is related to knee components misalignment that provokes abnormal stress distribution, in particular in the medial part of the polyethylene insert [6]. Furthermore, other studies have reported the role of the femoral-tibial torsion in pre-operative knees. In particular, the orthopaedists have observed that subjects with a tibial internal rotation between -16° and -9.1° seems to have a correlation with the OA development while those with a femoral-tibial torsion between -3° and -0.9° belong to the non-arthritic group [10]. In literature there are no studies on healthy knee, performed by means of FEA, in which are compered the effects of different femoral-tibial torsion configurations. For these reasons, this work aimed to develop two 3D knee prototype with a femoral-tibial torsion of -11°, referred as the internal rotation model, and 0°, referred as the external rotation model and which should represents the normal knee configuration. The results obtained from the FEA of the two models seem to be promising.

As shown in Figure 6.1 and Figure 6.2 the flexion is well replicated and from the rotation measurements on the applied Remote Point it has been found that the femur effectively performs a flexion of 40°. Furthermore, the femur external rotation was assessed and it has been found that during the flexion this rotation was equal to 3.4° in the internal rotation model and 4.6° in the external one. This is according to the screw-home mechanism, in which during the flexion there is also the internal rotation of the tibia or the external rotation of the femur. From the imposed Displacements on

the femur condyles this rotation was expected since the lateral displacement presented higher negative values. Actually, during real knee movement higher medial rotations can be achieved, in particular [43] states that during the first 40° of flexion occurs an internal rotation of the tibia about 11.40° ± 3.0°. This difference could be related to the chosen points of application of the Displacements on the femur condyles. But another study findings [44] are in line with the current work results, and then [45] reports that during the stance phase of gait only 5° of rotation around the longitudinal axis are performed. However, the lower value in the internal rotation model suggests that the movement will be concentrated in a narrow area provoking higher stresses onto the menisci and tibia.

In fact, Figure 6.3 presents the Maximum and Average von-Mises stress values on the menisci, in both models and at each considered flexion angle. The values related to the external rotation model seem to be validated in [38] which also used a force of -200 N in the analysis of the extension position. In the current work, it has been found a Maximum stress at 0° about 6.5 MPa and an Average stress near 0.34 MPa. These values are very similar to those found in [38] which report a Maximum value of 6.038 MPa and a mean stress value between two elements in the menisci of 0.303 MPa. Moreover, looking at the trend of the graphs (Figure 6.3) it can be said that the internal rotation model presents higher stress values in the menisci. Specifically, it can be observed that at 20° of flexion the internal rotation model presents a maximum stress of about 11 MPa against the almost 7 MPa of the external one. Moreover, it is well known that daily activities always imply flexions of at least 20°. This suggests that despite the static analysis does not account for the effects over time, it can be expected that a prolonged higher stress on the tibia will then leads to speed up the wear of knee cartilage.

This observation can be appreciated also in the graphical representations of the menisci stress from Figure 6.4 to Figure 6.8. As found in [28] the medial meniscus presents higher stress with respect to the lateral one. Additionally, looking at the flexion evolution can be noted that the stress moves posteriorly from a more anterior part, according to the roll-back movement as reported in [46].

Moreover, comparing the two representations the stress seems to be spread in a larger area in the internal rotation model. Finally in these representations, it is also confirmed the orthopaedist observation according to which the internal rotation model presents a stress concentrated in the middle of the medial meniscus, while in the external rotation model is more in the posterior part.

Instead, regarding the von-Mises stresses on the tibia of Figure 6.9, it can be observed the opposite trend. In fact, the external rotation model presents higher stress values with respect to the internal one. Nonetheless, in this case the difference among the two prototypes in the Maximum von-Mises stress is low. As seen in the menisci stress at 20° the internal rotation model is characterized by a peak value of 11 MPa. As said before, over time this could lead to menisci damage that will no more be able to transmit the stress to the tibia in the proper way. Thus, the tibia stress in the internal rotation model could get worse in the long run.

Anyhow, from a top view of the graphical representations of tibia stress (Figure 6.10 – 6.14) it seems clear that the virtual model with the femoral-tibial torsion of -11° exhibits a more extensive stress area, especially at 40° of flexion. Specifically, in the internal rotation model the stress reaches the middle part of the medial meniscus and this seems to explain the reported cases of varus configuration changes caused by the OA development [8]. Furthermore, these representations also confirm that greater flexion angles provoke an increase in the stress area in both models, as can be deduced from [47]. From the comparison among the two models, it can be evidenced that in the internal rotation case the stress reaches also the middle medial part of the tibia. The importance of this last observation can be better appreciated in Figure 6.15 in which the medial part of a real tibial cartilage and the two tibia stress representations at 40° are compared. Specifically, it seems that the medial wear of the real knee cartilage of a subject with OA is more compatible with the tibia stress present in the internal rotation model.

All the previous observations, and in particular the last one, are crucial to conclude that the orthopaedist observations seem to be confirmed from these simulations. Thus, from the analysed results it can be said that the internal rotation model is the worst condition that can be associated to an early development of OA. Despite these qualitative findings are in accordance with other works, the validation of all the obtained von-Mises stresses appears to be complicated. In fact, it is difficult to find comparable stress values due to the different considered conditions and set-up of other experiments [48].

In the present work, the choice related to the limited applied force was taken in order to facilitate the convergence of the simulation and to avoid an excessive increase of the computational time. Thus, the stress values obtained in this study tourn out to be smaller than other findings in which higher forces were considered [49][50]. However, it is assumed a linear increase of the stress with the increase of the axial force. In spite of this, the stress seems to be very close to the one reported in [38] which has considered the same force value. It is important to highlight that despite most studies used different conditions, the aim of the current work was to obtain a comparison among different configurations in order to determine which one provokes the worst stress distribution.

Of course, future works could improve the simulation in order to further validate the results and overcome the drawbacks of this study. In fact, the limitations of the current simulations are due to the chosen assumptions. In particular, the modelling of knee ligaments represents a crucial point, as found in literature [27]. They were modelled as linear elastic and isotropic unidimensional beams. Moreover, the bones were considered as homogeneous and linear elastic materials, thus neglecting their inhomogeneous behaviour due to the presence of cortical and cancellous parts. Furthermore, in the models the fibula and patella were not considered. Despite the representation of the first one is commonly avoided, the second one is important to perform a correct knee movement. However, due to the imposed kinematics, the patella action was considered with the previous described boundary conditions.

In summary, the current work has confirmed that the misalignment of the lower limbs, in particular the tibial internal rotation, provokes higher stress in the knee. As said before, this could be associated with the development of OA. Thus, the comparison among different configurations could be useful to determine the role of the osteotomy. It follows that the positively confirm of the orthopaedist observations provides a new role of the FEA on the knee virtual models. This means that the use of FEA could be useful in order to determine if an external rotation of the tibia performed by means of osteotomy, in a knee that present an internal femoral-tibial torsion, could provide significant improvement in the stress distribution of the knee. In addition, this evaluation could be helpful to delay the OA occurrence and thus postpone the prosthesis implantation and revision. Hence, prevention could play a key role in the health condition of the patient.

7 Conclusion

This thesis presents a finite element model to confirm the orthopaedist observation related to the effects of different femoral-tibial torsion configurations. The aim was successfully fulfilled and it has been found that the computational simulation of the internal rotation model exhibits worst stress values. In particular it has been confirmed that:

- The medial meniscus and the medial part of the tibia present the stress more in the middle part, in correspondence of the wear area observed by the orthopaedist;
- The internal rotation model (femoral-tibial torsion = -11°) presents a higher and a more spread stress with respect to the normal alignment configuration (femoral-tibial torsion = 0°).

Despite the results are promising, future studies could improve the models defined in this work. For instance, it could be developed models able to achieve greater flexion angles, simulating also different daily activities. Moreover, as seen from the literature, the modelling of the ligament behaviour has been long debated. In the present simulation they have been modelled as linear elastic and isotropic materials in order to simplify the prototype and to reduce the computational time. For the same purpose, knee bodies such as patella and fibula have been neglected. In particular, the lack of patella has been compensated considering its action by means of the applied boundary conditions, i.e. femoral condyles displacements. These drawbacks could be overcome for example modelling the ligaments as non-linear hyperelastic materials and including the omitted bodies.

In conclusion, despite the limitations, it seems that the employment of the FEA to compare different knee configurations could be useful to determine the benefits that preventive osteotomy could bring. In fact, the stress improvement that the external rotation of the tibia may provoke, could also delay the OA occurrence in subjects that tend to develop it, thus postponing also the TKA implantation and revision.

8 References

[1] R. Shenoy, P. S. Pastides, and D. Nathwani, "(iii) Biomechanics of the knee and TKR," *Orthop Trauma*, vol. 27, no. 6, pp. 364–371, Dec. 2013, doi: 10.1016/j.mporth.2013.10.003.

[2] S. Matsuda, S. E. White, V. G. Williams Ii, D. S. Mccarthy, and L. A. Whiteside, "Contact Stress Analysis in Meniscal Bearing Total Knee Arthroplasty," 1998.

[3] L. Farinelli, M. Baldini, A. Bucci, S. Ulisse, F. Carle, and A. Gigante, "Axial and rotational alignment of lower limb in a Caucasian aged non-arthritic cohort," *European Journal of Orthopaedic Surgery and Traumatology*, vol. 31, no. 2, pp. 221–228, Feb. 2021, doi: 10.1007/s00590-020-02763-7.

[4] J.-J. Liau, C.-K. Cheng, C.-H. Huang, and W.-H. Lo, "The effect of malalignment on stresses in polyethylene component of total knee prostheses-a finite element analysis." [Online]. Available: www.elsevier.com/locate/clinbiomech

[5] M. S. Zihlmann, A. Stacoff, J. Romero, I. Kramers-De Quervain, and E. Stüssi, "Biomechanical background and clinical observations of rotational malalignment in TKA:: Literature review and consequences," *Clinical Biomechanics*, vol. 20, no. 7, pp. 661–668, 2005, doi: 10.1016/j.clinbiomech.2005.03.014.

[6] K. Osano, R. Nagamine, M. Todo, and M. Kawasaki, "The effect of malrotation of tibial component of total knee arthroplasty on tibial insert during high flexion using a finite element analysis," *Scientific World Journal*, vol. 2014, 2014, doi: 10.1155/2014/695028.

[7] C. Planckaert, G. Larose, P. Ranger, M. Lacelle, A. Fuentes, and N. Hagemeister, "Total knee arthroplasty with unexplained pain: new insights

from kinematics," *Arch Orthop Trauma Surg*, vol. 138, no. 4, pp. 553–561, Apr. 2018, doi: 10.1007/s00402-018-2873-5.

[8] T. P. Andriacchi, P. L. Briant, S. L. Bevill, and S. Koo, "Rotational changes at the knee after ACL injury cause cartilage thinning," in *Clinical Orthopaedics and Related Research*, 2006, vol. 442, pp. 39–44. doi: 10.1097/01.blo.0000197079.26600.09.

[9] K. Kaneda *et al.*, "Increase in tibial internal rotation due to weight-bearing is a key feature to diagnose early-stage knee osteoarthritis: a study with upright computed tomography," *BMC Musculoskelet Disord*, vol. 23, no. 1, Dec. 2022, doi: 10.1186/s12891-022-05190-3.

[10] L. Farinelli *et al.*, "The Journal of Knee Surgery Surgical Epicondylar Axis of the Knee and Its Relationship to the Axial Tibia Alignment in Knee Osteoarthritis: The Concept of Proximal Twist Tibia 200683OA." [Online]. Available: https://www.thieme.de/en/thieme-connect/home-3939.htm.

[11] J. Sun *et al.*, "Finite element analysis of the valgus knee joint of an obese child," *Biomed Eng Online*, vol. 15, Dec. 2016, doi: 10.1186/s12938-016-0253-3.

[12] N. A. Z. Abidin, M. Rafiq Abdul Kadir, and M. H. Ramlee, "Three Dimensional Finite Element Modelling and Analysis of Human Knee Joint-Model Verification," in *Journal of Physics: Conference Series*, Nov. 2019, vol. 1372, no. 1. doi: 10.1088/1742-6596/1372/1/012068.

[13] J. F. Abulhasan and M. J. Grey, "Anatomy and physiology of knee stability," *Journal of Functional Morphology and Kinesiology*, vol. 2, no. 4. MDPI Multidisciplinary Digital Publishing Institute, Dec. 01, 2017. doi: 10.3390/jfmk2040034.

[14] J. Hashemi *et al.*, "The geometry of the tibial plateau and its influence on the biomechanics of the tibiofemoral joint," *Journal of Bone and Joint Surgery*, vol. 90, no. 12, pp. 2724–2734, Dec. 2008, doi: 10.2106/JBJS.G.01358.

[15] Y. Dong, Y. Dong, Q. Xu, G. Hu, and W. Dong, "The effect of varying degrees of radial meniscal tears on the knee contact stresses: A finite element analysis,"

in *Advanced Materials Research*, 2011, vol. 304, pp. 135–141. doi: 10.4028/www.scientific.net/AMR.304.135.

[16] S. L. Y. Woo, S. D. Abramowitch, R. Kilger, and R. Liang, "Biomechanics of knee ligaments: Injury, healing, and repair," *Journal of Biomechanics*, vol. 39, no. 1. pp. 1–20, 2006. doi: 10.1016/j.jbiomech.2004.10.025.

[17] F. Flandry and G. Hommel, "Normal Anatomy and Biomechanics of the Knee," 2011. [Online]. Available: www.sportsmedarthro.com

[18] J. R. Robinson, A. M. J. Bull, R. R. D. W. Thomas, and A. A. Amis, "The role of the medial collateral ligament and posteromedial capsule in controlling knee laxity," *American Journal of Sports Medicine*, vol. 34, no. 11, pp. 1815–1823, Nov. 2006, doi: 10.1177/0363546506289433.

[19] J. W. Jeon and J. Hong, "Comparison of screw-home mechanism in the unloaded living knee subjected to active and passive movements," *J Back Musculoskelet Rehabil*, vol. 34, no. 4, pp. 589–595, 2021, doi: 10.3233/BMR-200110.

[20] V. Pinskerova *et al.*, "Does the femur roll-back with flexion?," vol. 86, no. 6, 2004, doi: 10.1302/0301-620X.86B6.

[21] M. M. Wachowski *et al.*, "Total knee replacement with natural rollback," *Annals of Anatomy*, vol. 194, no. 2, pp. 195–199, Mar. 2012, doi: 10.1016/j.aanat.2011.01.013.

[22] S. D. Masouros and A. M. J. Bull, "(i) Biomechanics of the knee joint."

[23] P. Sarzi-Puttini *et al.*, "Osteoarthritis: An overview of the disease and its treatment strategies," *Seminars in Arthritis and Rheumatism*, vol. 35, no. 1 SUPPL. 1. pp. 1–10, Aug. 2005. doi: 10.1016/j.semarthrit.2005.01.013.

[24] J. W. P. Michael, K. U. Schlüter-Brust, and P. Eysel, "Epidemiologie, ätiologie, diagnostik und therapie der gonarthrose," *Deutsches Arzteblatt*, vol. 107, no. 9. pp. 152–162, Mar. 05, 2010. doi: 10.3238/arztebl.2010.0152.

[25] L. Zabawa, K. Li, and S. Chmell, "Patient dissatisfaction following total knee arthroplasty: external validation of a new prediction model," *European Journal*

of Orthopaedic Surgery and Traumatology, vol. 29, no. 4, pp. 861–867, May 2019, doi: 10.1007/s00590-019-02375-w.

[26] A. Postler, C. Lützner, F. Beyer, E. Tille, and J. Lützner, "Analysis of Total Knee Arthroplasty revision causes," *BMC Musculoskelet Disord*, vol. 19, no. 1, Feb. 2018, doi: 10.1186/s12891-018-1977-y.

[27] F. Galbusera *et al.*, "Material models and properties in the finite element analysis of knee ligaments: A literature review," *Frontiers in Bioengineering and Biotechnology*, vol. 2, no. NOV. Frontiers Media S.A., 2014. doi: 10.3389/fbioe.2014.00054.

[28] K. Kumar and V. Acharya, "Finite Element Analysis of a Human Knee Joint." [Online]. Available: https://www.researchgate.net/publication/309320993

[29] A. Fottner *et al.*, "Impact of tibial baseplate malposition on kinematics, contact forces and ligament tensions in TKA: A numerical analysis," *J Mech Behav Biomed Mater*, vol. 103, Mar. 2020, doi: 10.1016/j.jmbbm.2019.103564.

[30] S. Kuriyama, M. Ishikawa, M. Furu, H. Ito, and S. Matsuda, "Malrotated tibial component increases medial collateral ligament tension in total knee arthroplasty," *Journal of Orthopaedic Research*, vol. 32, no. 12, pp. 1658–1666, Dec. 2014, doi: 10.1002/jor.22711.

[31] B. Innocenti, J. Bellemans, and F. Catani, "Deviations From Optimal Alignment in TKA: Is There a Biomechanical Difference Between Femoral or Tibial Component Alignment?," *Journal of Arthroplasty*, vol. 31, no. 1, pp. 295–301, Jan. 2016, doi: 10.1016/j.arth.2015.07.038.

[32] B. Innocenti and E. Bori, "Change in knee biomechanics during squat and walking induced by a modification in TKA size," *J Orthop*, vol. 22, pp. 463–472, Nov. 2020, doi: 10.1016/j.jor.2020.10.006.

[33] Z. Trad, A. Barkaoui, M. Chafra, and J. M. R. S. Tavares, "Finite element models of the knee joint," in *SpringerBriefs in Applied Sciences and Technology*,

no. 9783319741574, Springer Verlag, 2018, pp. 1–34. doi: 10.1007/978-3-319-74158-1_1.

[34] E. Peña, B. Calvo, M. A. Martínez, D. Palanca, and M. Doblaré, "Finite element analysis of the effect of meniscal tears and meniscectomies on human knee biomechanics," *Clinical Biomechanics*, vol. 20, no. 5, pp. 498–507, 2005, doi: 10.1016/j.clinbiomech.2005.01.009.

[35] M. Woiczinski, A. Steinbrück, P. Weber, P. E. Müller, V. Jansson, and C. Schröder, "Development and validation of a weight-bearing finite element model for total knee replacement," *Comput Methods Biomech Biomed Engin*, vol. 19, no. 10, pp. 1033–1045, Jul. 2016, doi: 10.1080/10255842.2015.1089534.

[36] X. Wu, B. Pei, W. Wang, D. Lu, L. Guo, and P. He, "Finite element analysis of a novel approach for knee and ankle protection during landing," *Applied Sciences (Switzerland)*, vol. 11, no. 4, pp. 1–12, Feb. 2021, doi: 10.3390/app11041912.

[37] G. A. Orozco, P. Tanska, M. E. Mononen, K. S. Halonen, and R. K. Korhonen, "The effect of constitutive representations and structural constituents of ligaments on knee joint mechanics," *Sci Rep*, vol. 8, no. 1, Dec. 2018, doi: 10.1038/s41598-018-20739-w.

[38] P. K. Subbukrishnan, P. Kumar, R. Kandadai, P. G. Student, and V. Professor, "FINITE ELEMENT MODELING OF HUMAN KNEE JOINT-MENISCUS UNDER COMPRESSIVE LOAD," 2015. [Online]. Available: https://www.researchgate.net/publication/275016828

[39] K. Kono *et al.*, "Femoral rollback at high-flexion during squatting is related to the improvement of sports activities after bicruciate-stabilized total knee

arthroplasty: an observational study," *BMC Musculoskelet Disord*, vol. 23, no. 1, Dec. 2022, doi: 10.1186/s12891-022-05464-w.

[40] K. Murakami *et al.*, "Knee kinematics in bi-cruciate stabilized total knee arthroplasty during squatting and stair-climbing activities," *J Orthop*, vol. 15, no. 2, pp. 650–654, Jun. 2018, doi: 10.1016/j.jor.2018.05.003.

[41] D. Shah, T. Bates, C. Kampfer, and D. Hope, "Biomechanics and Outcomes of Modern Tibial Polyethylene Inserts," 2022, doi: 10.1007/s12178-022-09755-6/Published.

[42] P. Johal, A. Williams, P. Wragg, D. Hunt, and W. Gedroyc, "Tibio-femoral movement in the living knee. A study of weight bearing and non-weight bearing knee kinematics using 'interventional' MRI," *J Biomech*, vol. 38, no. 2, pp. 269–276, Feb. 2005, doi: 10.1016/j.jbiomech.2004.02.008.

[43] H. N. Chen, K. Yang, Q. R. Dong, and Y. Wang, "Assessment of tibial rotation and meniscal movement using kinematic magnetic resonance imaging," *J Orthop Surg Res*, vol. 9, no. 1, Aug. 2014, doi: 10.1186/s13018-014-0065-8.

[44] G. Li, C. Zhou, Z. Zhang, T. Foster, and H. Bedair, "Articulation of the femoral condyle during knee flexion," *J Biomech*, vol. 131, Jan. 2022, doi: 10.1016/j.jbiomech.2021.110906.

[45] M. A. R. Freeman and V. Pinskerova, "The movement of the normal tibio-femoral joint," *J Biomech*, vol. 38, no. 2, pp. 197–208, 2005, doi: 10.1016/j.jbiomech.2004.02.006.

[46] K. Zhang *et al.*, "The biomechanical changes of load distribution with longitudinal tears of meniscal horns on knee joint: A finite element analysis," *J Orthop Surg Res*, vol. 14, no. 1, Jul. 2019, doi: 10.1186/s13018-019-1255-1.

[47] B. Innocenti, S. Pianigiani, L. Labey, J. Victor, and J. Bellemans, "Contact forces in several TKA designs during squatting: A numerical sensitivity analysis," *J Biomech*, vol. 44, no. 8, pp. 1573–1581, May 2011, doi: 10.1016/j.jbiomech.2011.02.081.

[48] N. H. Yang, P. K. Canavan, H. Nayeb-Hashemi, B. Najafi, and A. Vaziri, "Protocol for constructing subject-specific biomechanical models of knee joint,"

Comput Methods Biomech Biomed Engin, vol. 13, no. 5, pp. 589–603, 2010, doi: 10.1080/10255840903389989.

[49] A. Mestar, S. Zahaf, N. Zina, and A. Boutaous, "Development and validation of a numerical model for the mechanical behavior of knee prosthesis analyzed by the finite elements method," *Journal of Biomimetics, Biomaterials and Biomedical Engineering*, vol. 37, pp. 12–42, 2018, doi: 10.4028/www.scientific.net/JBBBE.37.12.

[50] R. Rai and V. Rastogi, "Dynamic(Explicit) analysis(FEA) of the knee joint during Knee flexion movement."